脉冲星计时阵列简介及超轻暗物质探测

夏子晴

中国科学院紫金山天文台

南京师范大学，紫金山暗物质研讨会

2023年12月31日

Outline

1. 脉冲星计时阵列简介
2. TOA数据及噪声模型
3. 超轻暗物质间接探测

Outline

1. 脉冲星计时阵列简介

2. TOA数据及噪声模型

3. 超轻暗物质间接探测

Millisecond pulsar (MSP)

- Rotation period ~ ms, below 10 ms;
  Old neutron star ~ billion years;
  Very small magnetic field strength.
- Very high binary fraction (>50%, white dwarf companion)
- Detected in radio, X-ray, and gamma-ray
- **Most accurate and stable clocks in space**

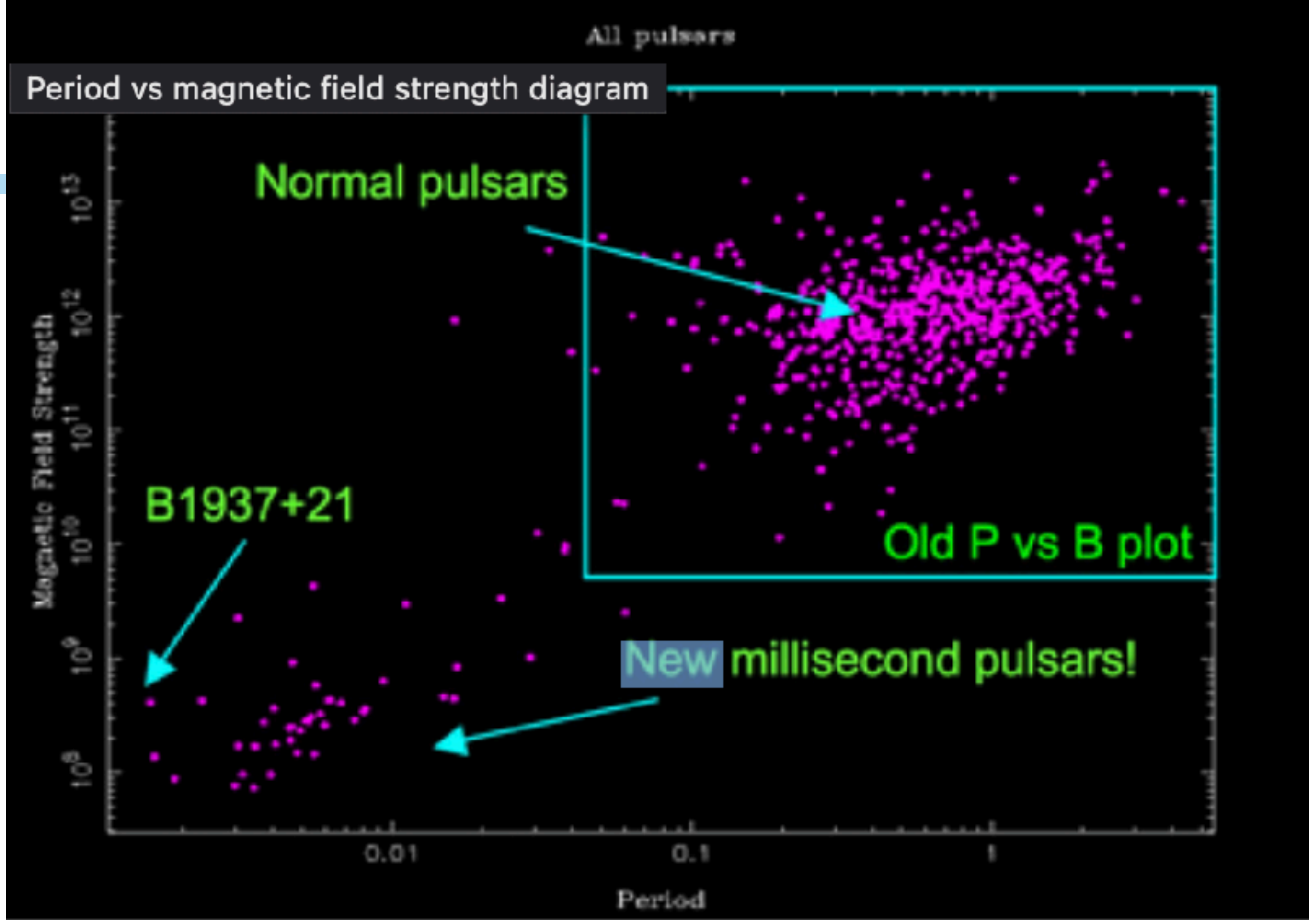

J0614.1-3329 Pulse Phase (Fermi-LAT)

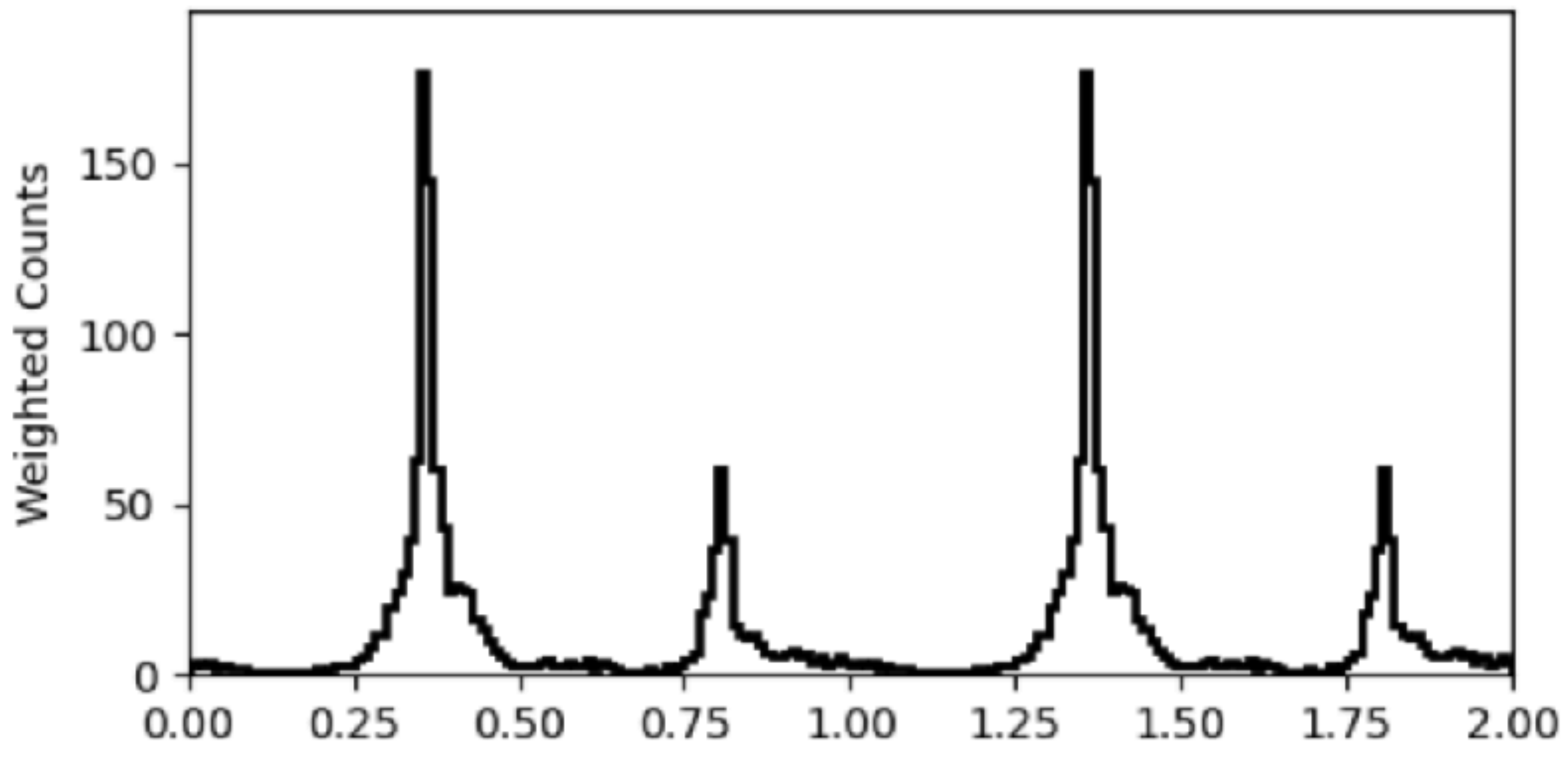

Pulsar Timing Array (PTA)

- **An array of galactic MSPs with extremely high rotational stability** are originally proposed to detect **nanohertz gravitational waves** with **the Time of Arrival (TOA)** for the MSPs pulses.

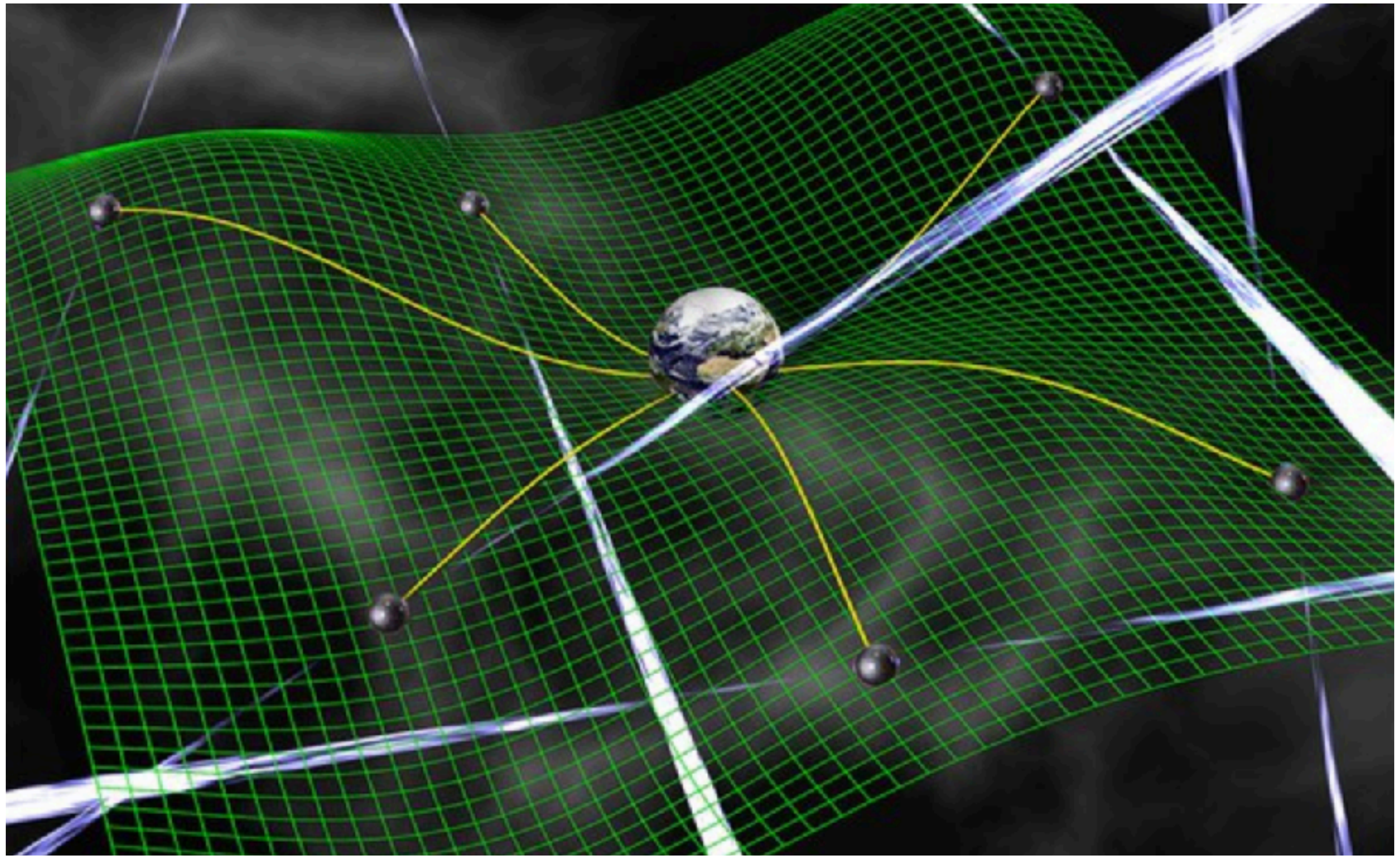

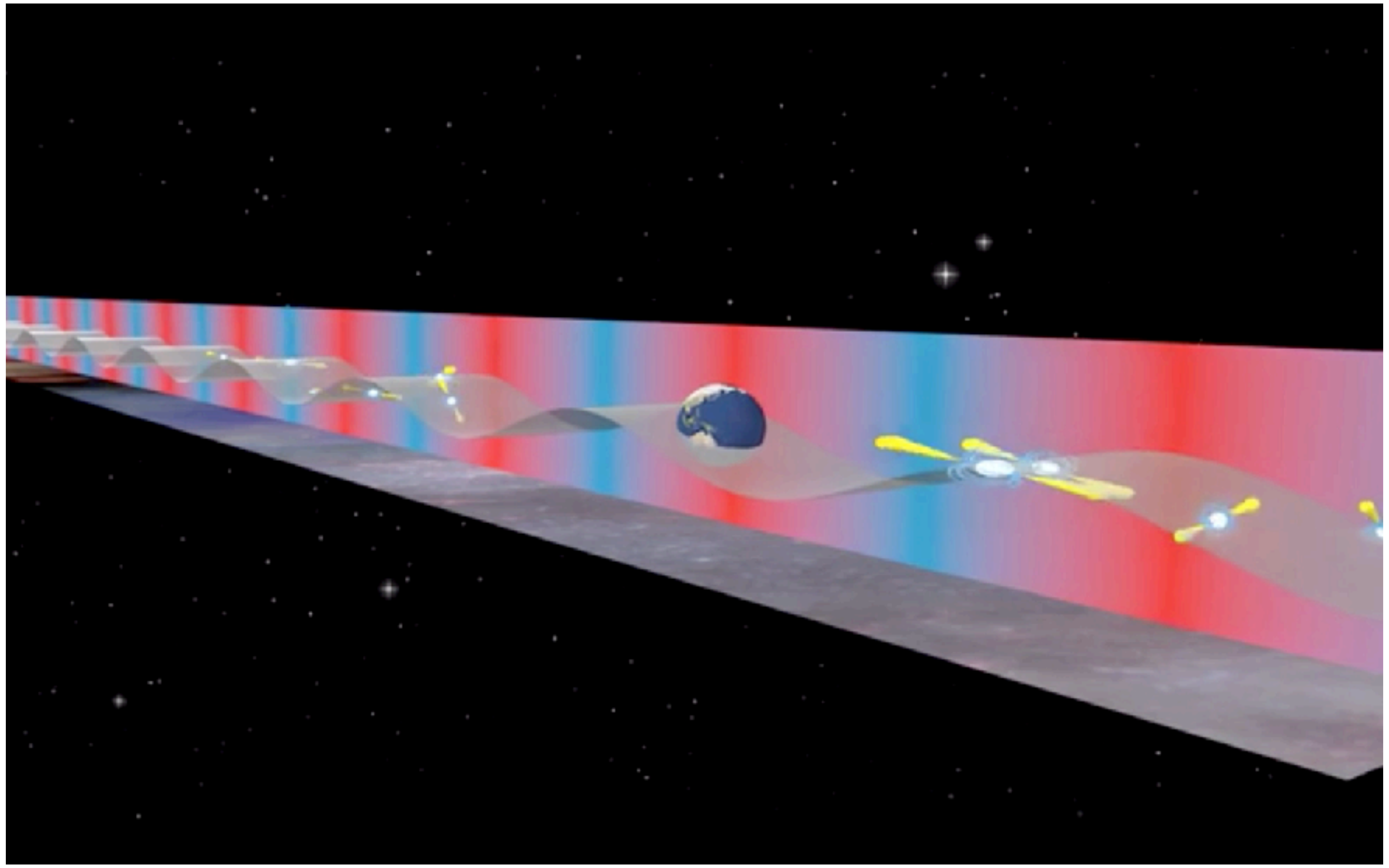

Credit: B. Saxton (NRAO/AUI/NSF)

Radio Pulsar Timing Array

IPTA DR2 (2019) IPTA DR3 ~ 85MSP upcoming

- **65** millisecond pulsars with high-precision timing data.

PTA	Telescope	Typical cadence (weeks)	No. of pulsars	Observing Frequencies (GHz)	Data span (MJD/Gregorian) Earliest—Latest
EPTA	EFF	4	18	1.4, 2.6	50360 (1996 Oct 04) – 56797 (2014 May 20)
	JBO	3	35	1.4	54844 (2009 Jan 13) – 57028 (2015 Jan 06)
	NRT	2	42	1.4, 2.1	47958 (1990 Mar 08) – 56810 (2014 Jun 02)
	WSRT	4	19	0.3, 1.4, 2.2	51386 (1999 Jul 27) – 55375 (2010 Jun 28)
NANOGrav	GBT	4	20	0.8, 1.4	53216 (2004 Jul 30) – 56598 (2013 Nov 02)
	AO	4	19	0.3, 0.4, 1.4, 2.3	53343 (2004 Dec 04) – 56599 (2013 Nov 03)
Zhu et al. (2015)	GBT and AO	2	1	0.8, 1.4, 2.3	48850 (1992 Aug 16) – 56598 (2013 Nov 02)
Kaspi et al. (1994)	AO	2	2	1.4, 2.3	46436 (1986 Jan 06) – 48973 (1992 Dec 17)
PPTA	PKS	2	20	0.6, 1.4, 3.1	49373 (1994 Jan 21) – 57051 (2015 Jan 29)

(https://gitlab.com/IPTA/DR2/tree/master/release)

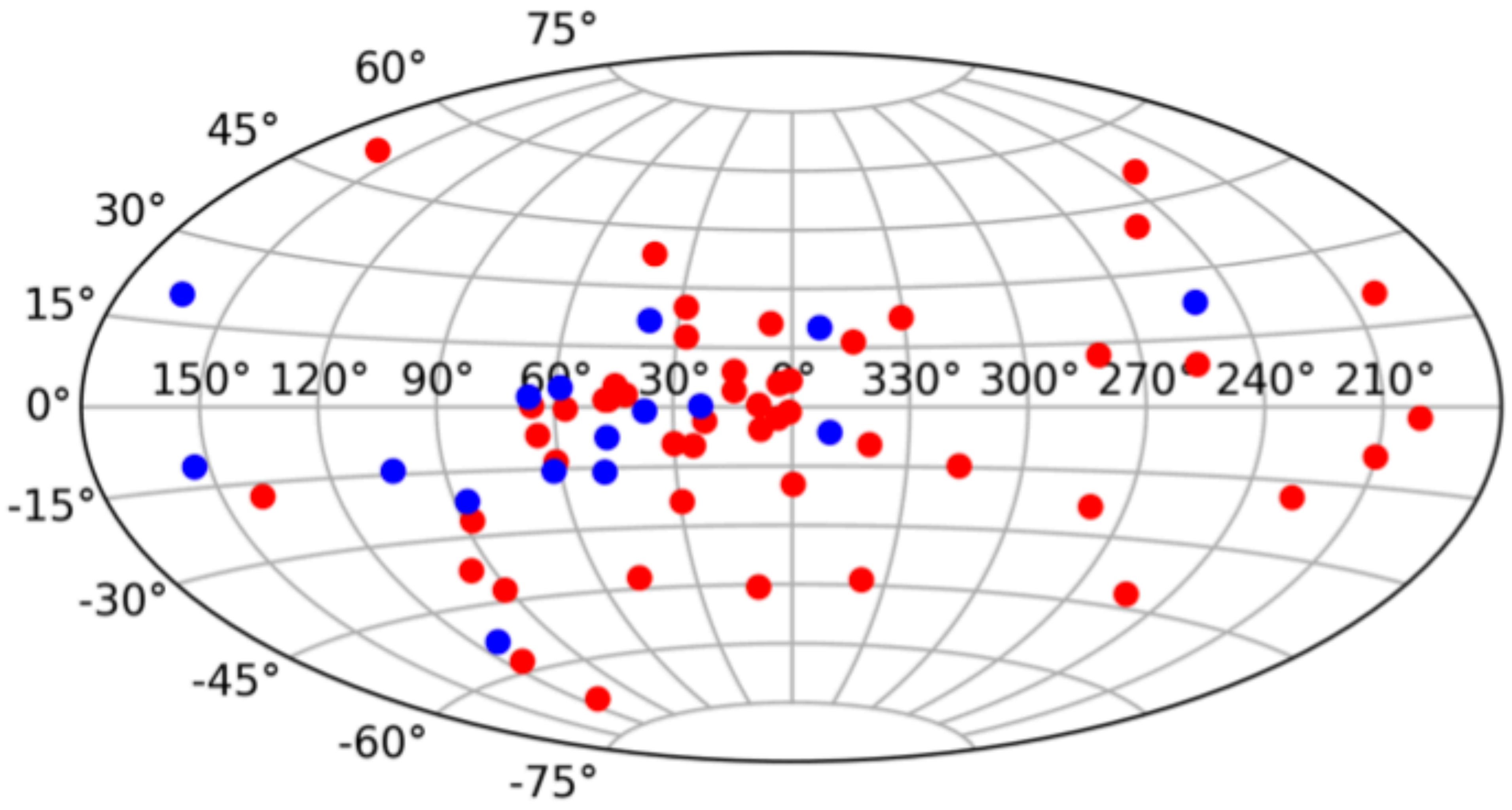

Red: DR1-2016 (49)
Blue: new in DR2-2019 (16)

B. B. P. Perera et al.,arXiv:1909.04534

https://gwac.wvu.edu/blog/2018/05/01/international-pulsar-timing-array-student-workshop-and-science-meeting-june-2018

CPTA DR1

FAST

3.5 yr

57 MSP

~10纳秒

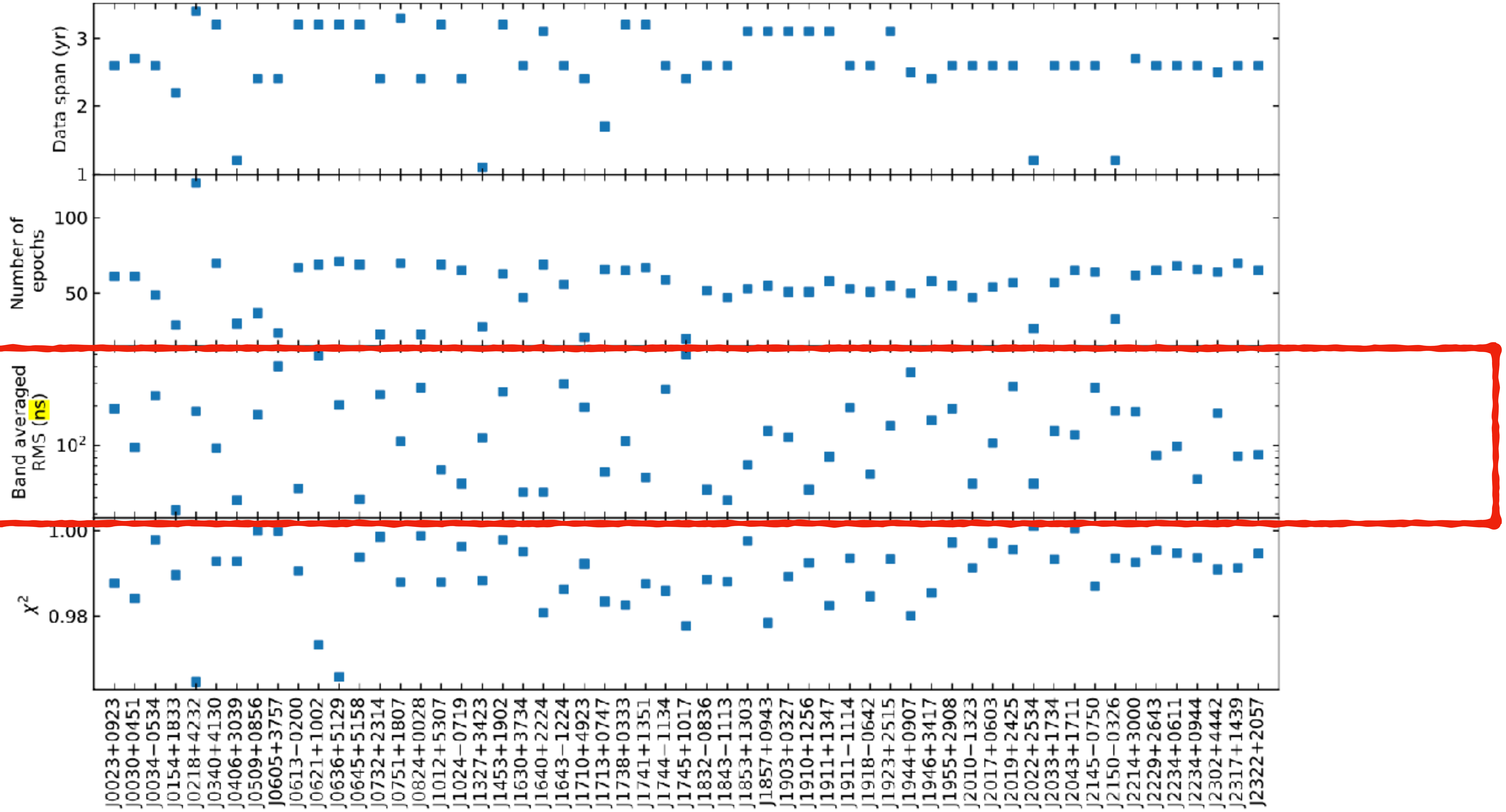

Fig. 1: Summary of the CPTA DR1 data quality. From top to bottom, the panels show data span, number of epochs, weighted root-mean-square (RMS) of frequency integrated residuals, and reduced χ^2 of timing residual, respectively.

NanoGrav 15yr data (NG15)

- 68 millisecond pulsars (MSPs) observed monthly
- Time span ~15 yr (2004-2020 maximum 16yr)
- Add 21 MSPs and extend 3 yr (对比 DR4-NG12.5yr)
- narrowband data set ~ 676,465 TOAs
  wideband data set ~20,290 TOAs
- 100 m Green Bank Telescope
  305 m Arecibo Observatory (until 2020)
  27 25 m antennae of the VLA (from 2015, new 6 MSPs)
  (327Mhz ~ 3Ghz)
- entirely PINT-based timing analysis (PINT_Pal)

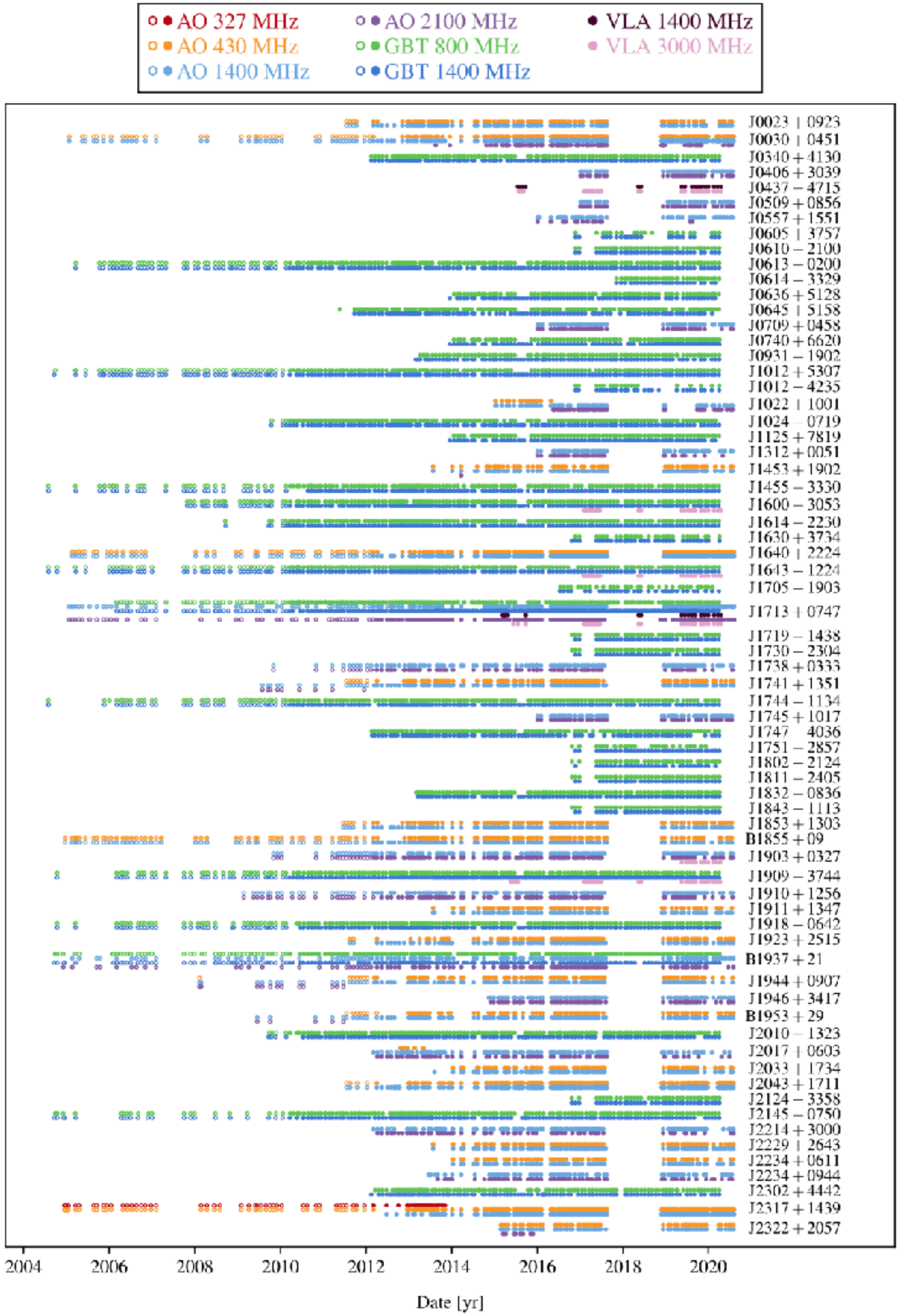

GW - Pulsar Timing Array (PTA)

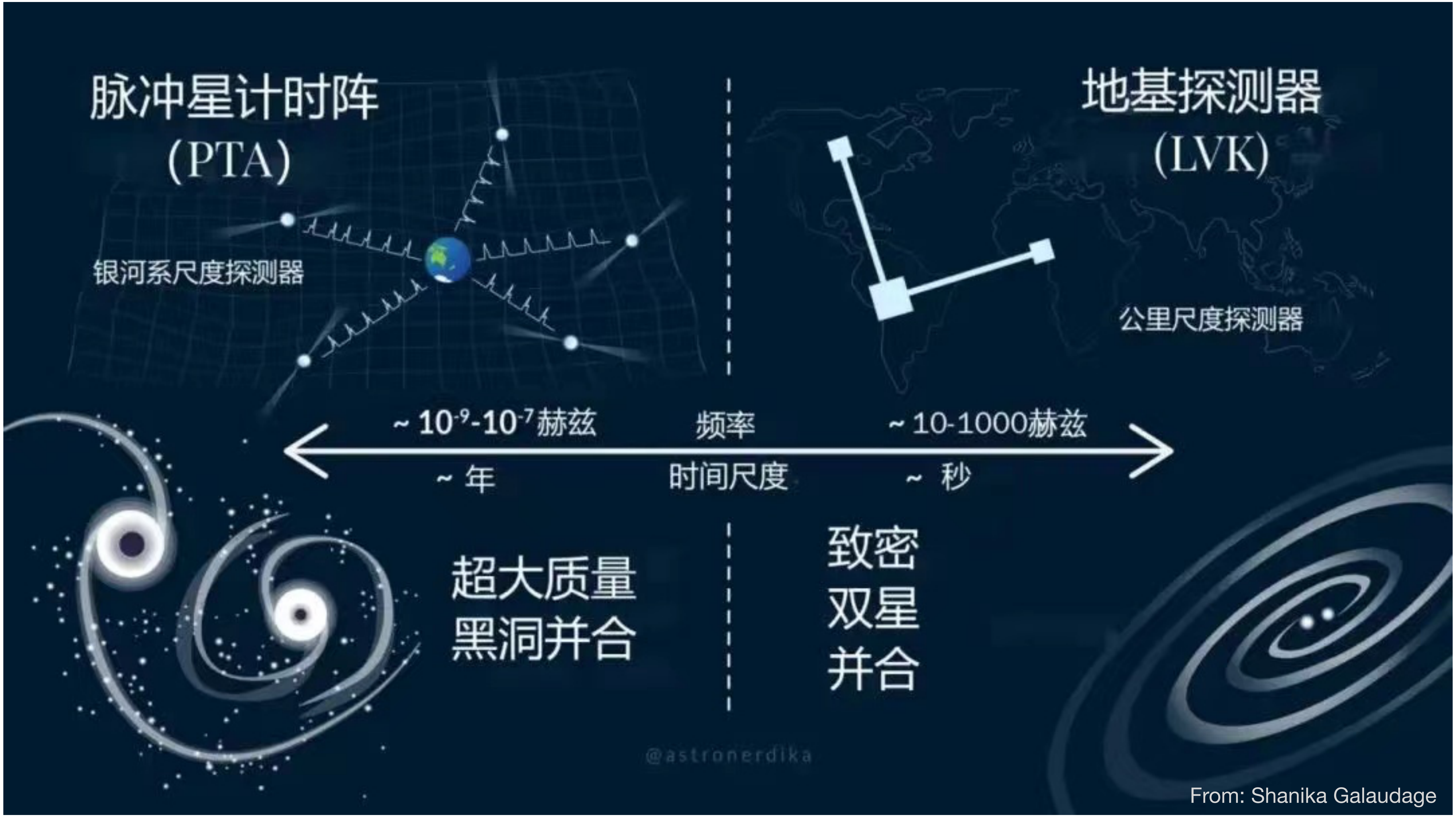

GWB - Radio PTA (2023.6 一起发布)

NANOGrav NG15	15 yr 68 MSP ~百纳秒	**GWB ~ 4.0 sigma**
EPTA + InPTA DR2	24 yr 25 MSP ~百纳秒	**GWB ~ 3.3 sigma**
PPTA DR3	18 yr 32 MSP ~百纳秒	**GWB ~ 2.2 sigma**
CPTA DR1	3.5 yr 57 MSP ~10纳秒	**GWB ~ 4.6 sigma**

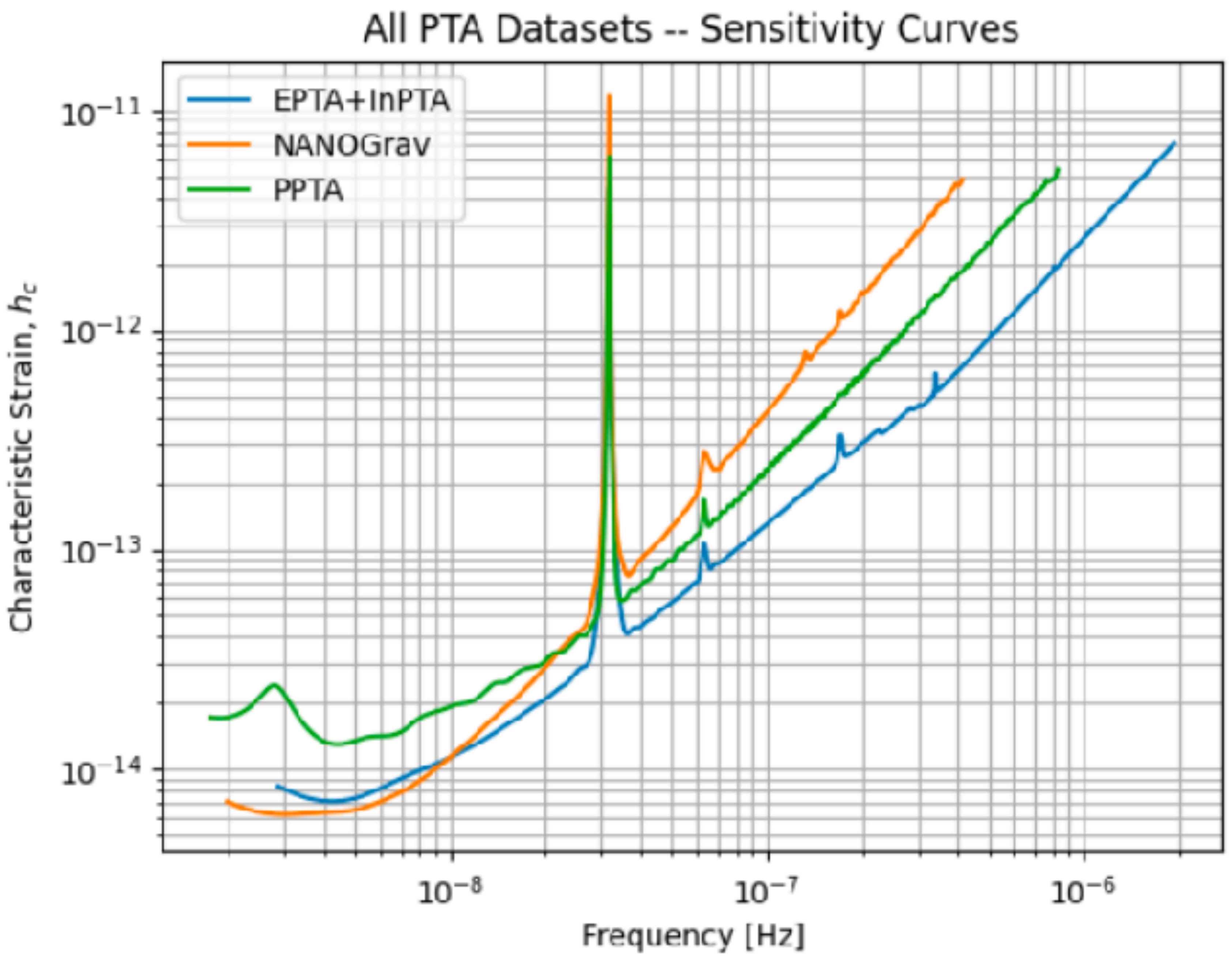

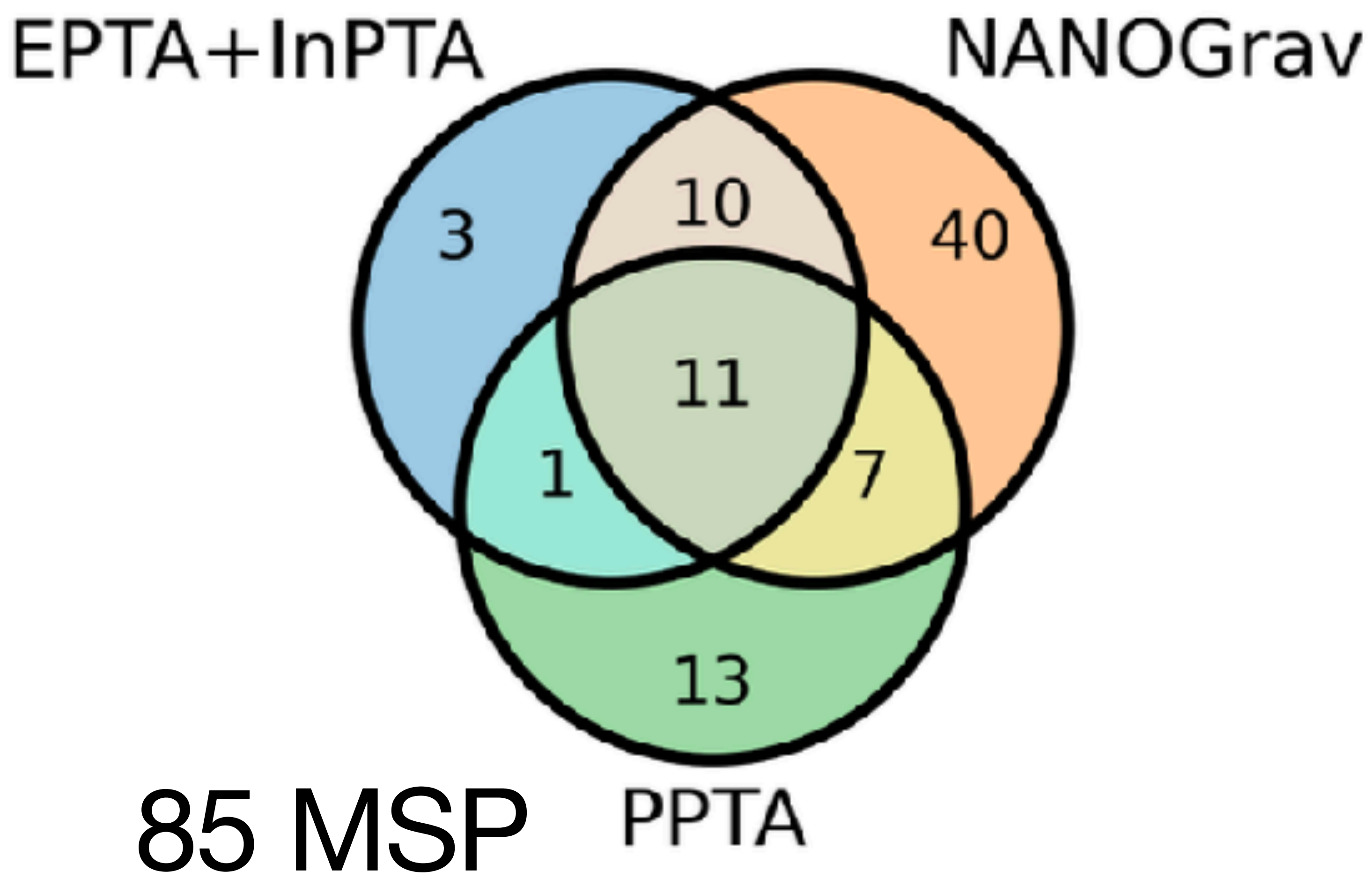

85 MSP

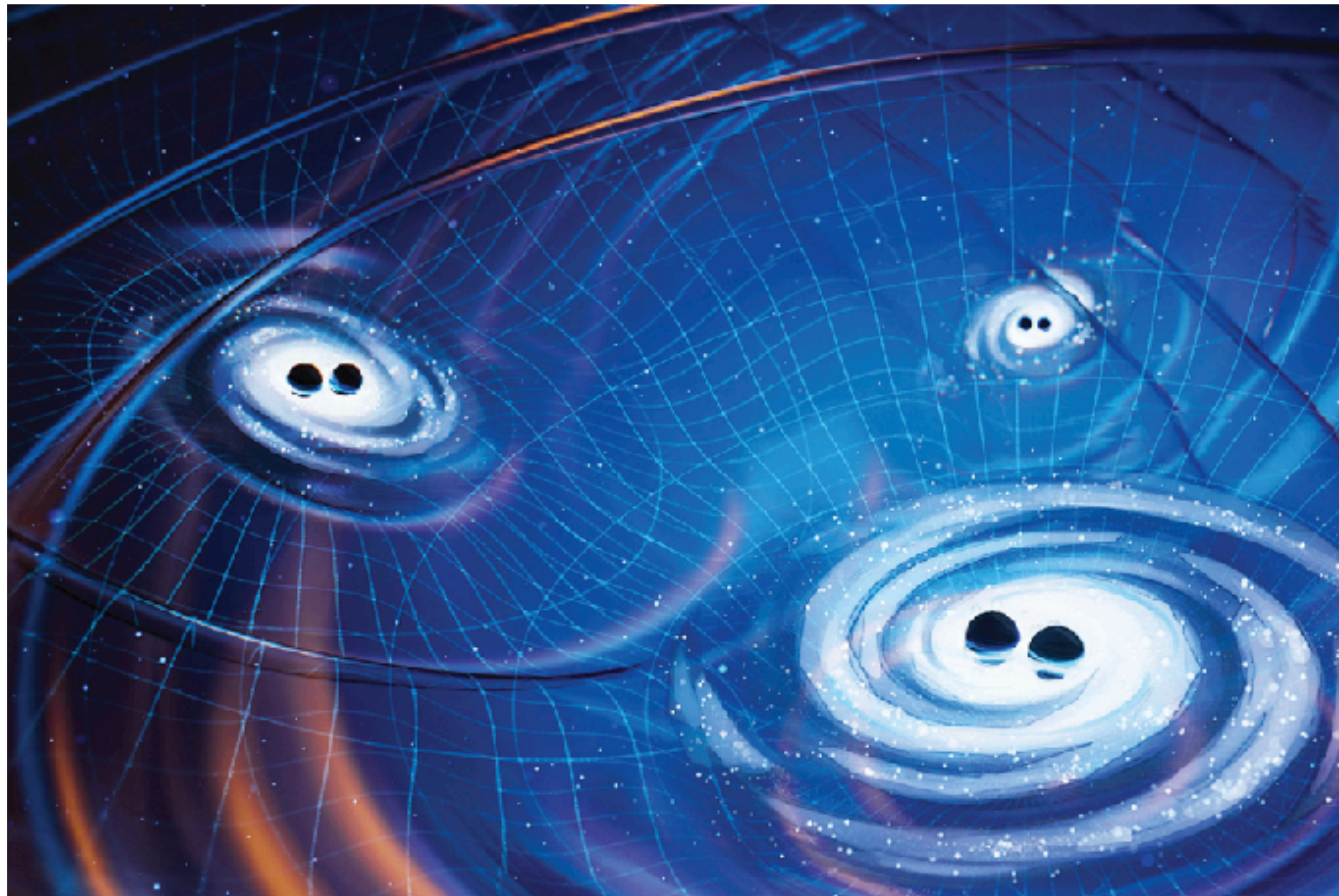

GWB - Radio PTA

GWB $$\Gamma_{ab}^{\rm HD} = \frac{1}{2}\delta_{ab} + \frac{3}{2}x_{ab}\ln x_{ab} - \frac{1}{4}x_{ab} + \frac{1}{2},$$ 引力波经过地球 - 垂直方向上符号相反（四极矩）

GWB - Gamma-ray PTA

Fermi-LAT PTA: New Pulsar Timing Array with the Gamma-ray observation.

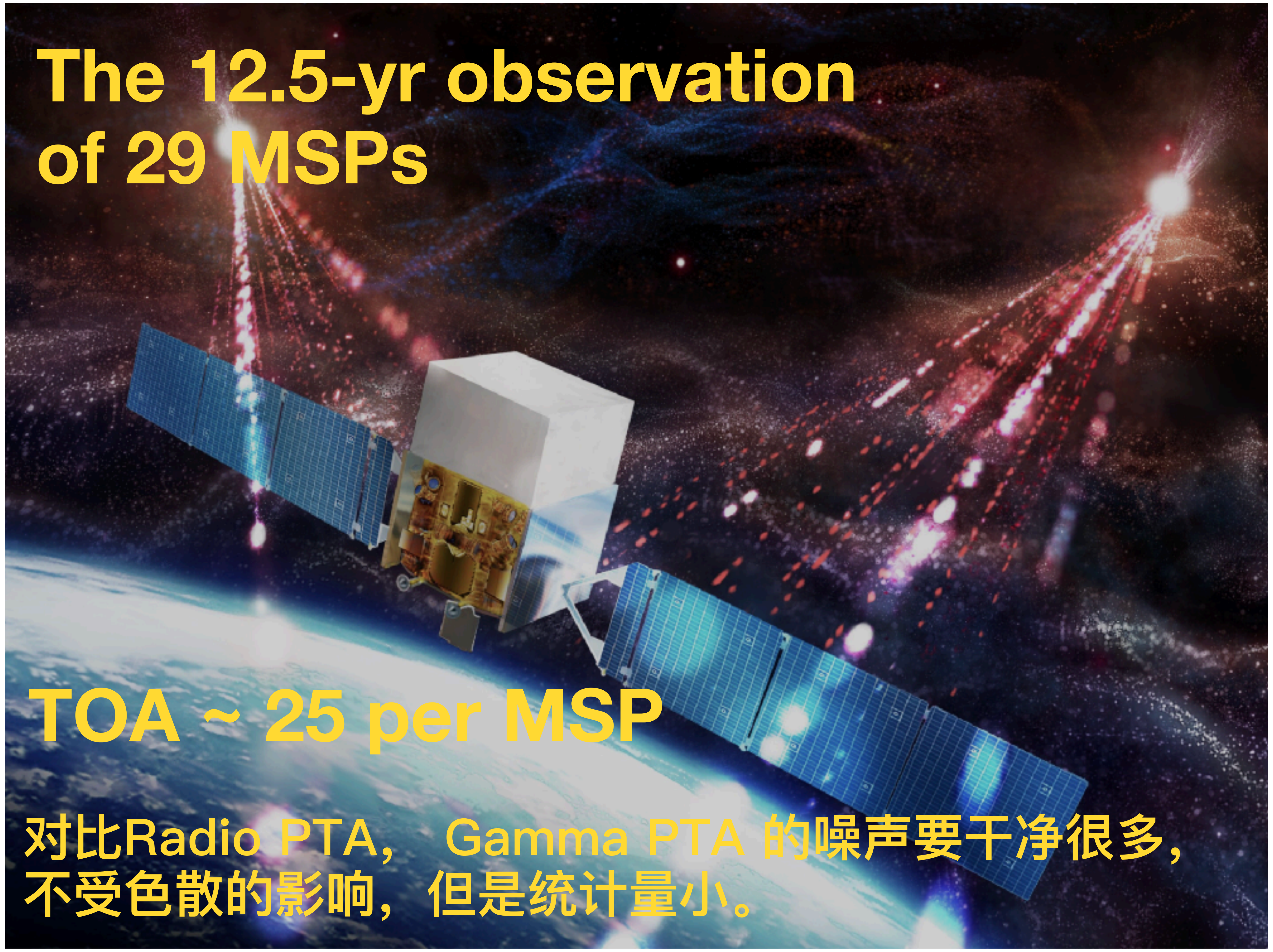

Pulsar Name (PSR)	Cadence (ToA/yr)	d_p (kpc)	σ_{ToA} (μs)	rms (μs)	Noise Model (favored)
J0030+0451	2	0.32	4.13	4.32	None[b]
J0034−0534	2	1.35	13.41	10.11	None
J0101−6422	2	1.00	14.16	16.85	None
J0102+4839	2	2.31	16.14	19.18	None
J0340+4130	2	1.60	18.26	23.03	None
J0533+6759	1.5	2.40	16.80	13.30	None
J0613−0200	2	0.78	19.41	14.46	None
J0614−3329	2	0.63	2.53	2.71	None
J0740+6620	1.5	1.15	10.53	2.34	None
J1124−3653	2	0.99	10.33	3.13	None
J1231−1411	2	0.42	2.43	2.51	None
J1514−4946	2	0.91	12.48	14.22	None
J1536−4948	2	0.98	7.02	7.01	None
J1614−2230	2	0.70	5.80	10.35	None
J1625−0021	1.5	0.95	18.52	15.27	None
J1630+3734	2	1.19	5.82.	5.64	None
J1810+1744	2	2.36	10.26	12.44	None
J1816+4510	2	4.36	19.72	25.01	None
J1858−2216	2	0.92	13.10	19.05	None
J1902−5105	2	1.65	7.84	7.62	None
J1939+2134	1.5	3.50	7.20	11.45	None
J1959+2048	2	1.40	4.78	9.35	WN
J2017+0603	2	1.40	14.38	19.94	None
J2034+3632	1.5	–	17.59	18.73	None
J2043+1711	2	1.39	8.04	9.29	None
J2214+3000	2	0.60	20.09	23.94	None
J2241−5236	2	1.04	5.30	6.57	WN
J2256−1024	1.5	2.08	4.13	5.23	None
J2302+4442	2	0.86	11.38	8.20	None

GWB - Gamma-ray PTA

Science REPORTS

Cite as: The Fermi-LAT Collaboration, *Science* 10.1126/science.abm3231 (2022).

A gamma-ray pulsar timing array constrains the nanohertz gravitational wave background

The Fermi-LAT Collaboration*†

*Fermi-LAT Collaboration authors and affiliations are listed in the supplementary materials.

†Corresponding authors: Matthew Kerr (matthew.kerr@gmail.com); Aditya Parthasarathy (adityapartha311

After large galaxies merge, their central supermassive black holes are exp
Their orbital motion should generate a gravitational wave background (GW
Searches for this background utilize pulsar timing arrays, which perform l
millisecond pulsars at radio wavelengths. We use 12.5 years of Fermi Large
gamma-ray pulsar timing array. Results from 35 bright gamma-ray pulsars
GWB characteristic strain of 1.0 × 10^{-14} at a frequency of 1 yr^{-1}. The sensiti
the observing time span, as $t_{obs}^{-13/6}$. This direct measurement provides an ind
offering a check on radio noise models.

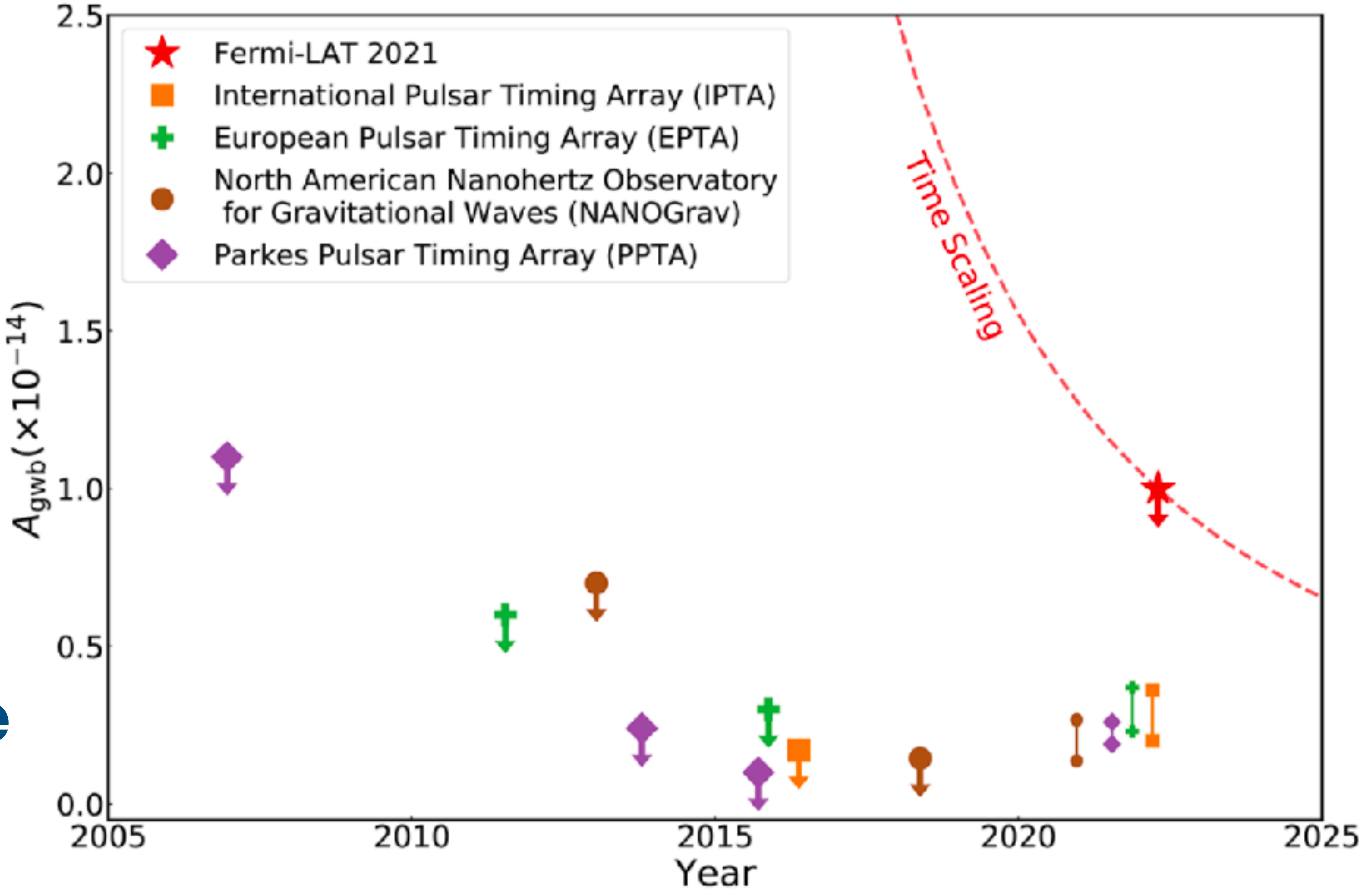

Fermi will reach a sensitivity comparable to radio PTA in 5 to 10 years.

Outline

1. 脉冲星计时阵列简介

2. **TOA数据及噪声模型**

3. 超轻暗物质间接探测

TOA数据及噪声模型

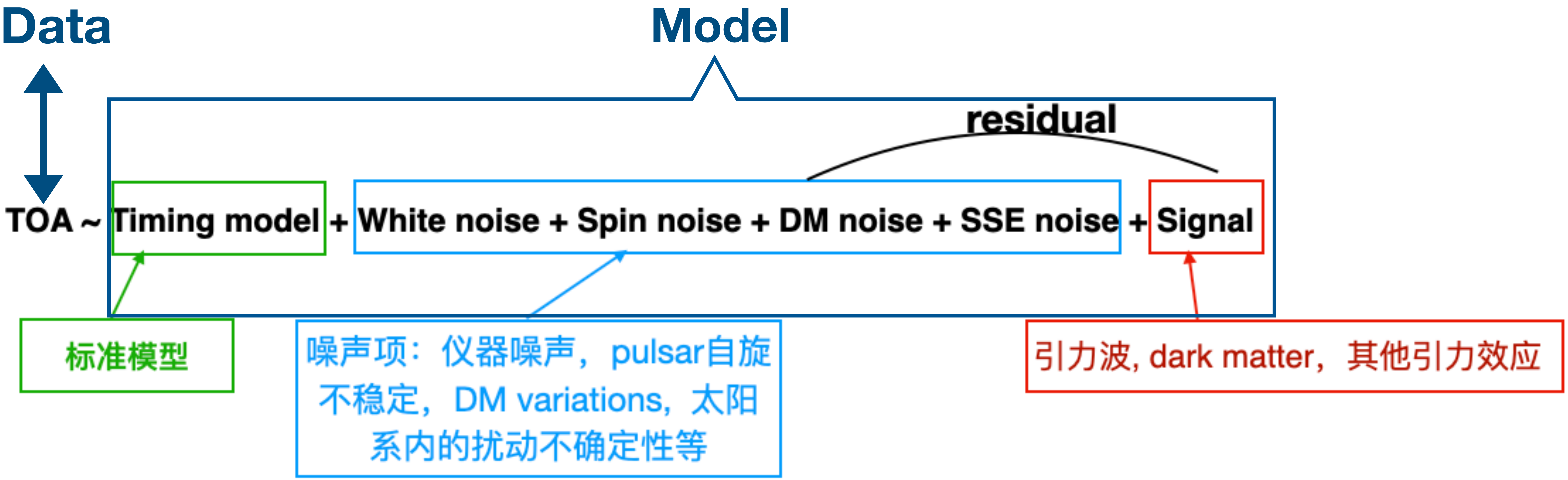

- Likelihood analysis

$$\mathcal{L}(\boldsymbol{\delta t}|\boldsymbol{\theta}) = \frac{\exp\left(-\frac{1}{2}(\boldsymbol{\delta t}-\boldsymbol{\mu})^T \boldsymbol{C}^{-1}(\boldsymbol{\delta t}-\boldsymbol{\mu})\right)}{\sqrt{\det\left(2\pi \boldsymbol{C}\right)}},$$

- Signal 和 noise是相对的，取决于研究目标

TOA data

TOA data 保存在tim文件

NANOGrav

```
53358.000056.3.000.000.9y.x.ff 424.000000 53358.767912764015642   1.277  ao  -fe 430 -be ASP -f 430_ASP -bw 4 -
    tobs 903.18 -tmplt B1855+09.430.PUPPI.9y.x.sum.sm -gof 1.09 -nbin 2048 -nch 1 -chan 1 -subint 0 -snr 142.71
    -wt 15 -proc 9y -pta NANOGrav -to -0.789e-6
53358.000056.3.000.000.9y.x.ff 428.000000 53358.767912759999400   0.858  ao  -fe 430 -be ASP -f 430_ASP -bw 4 -
    tobs 903.18 -tmplt B1855+09.430.PUPPI.9y.x.sum.sm -gof 1.13 -nbin 2048 -nch 1 -chan 2 -subint 0 -snr 207.92
    -wt 15 -proc 9y -pta NANOGrav -to -0.789e-6
```

mock data

名称	射电频率	TOA	TOA误差	观测坐标
c01_J0030+0451	1440.00000000	53000.0000000074400930	0.10000	AXIS
c01_J0030+0451	1440.00000000	53013.99999997887108094	0.10000	AXIS
c01_J0030+0451	1440.00000000	53028.00000000331760930	0.10000	AXIS
c01_J0030+0451	1440.00000000	53041.99999999927825911	0.10000	AXIS
c01_J0030+0451	1440.00000000	53056.00000000455563764	0.10000	AXIS
c01_J0030+0451	1440.00000000	53070.00000001754843382	0.10000	AXIS
c01_J0030+0451	1440.00000000	53084.00000000073177375	0.10000	AXIS
c01_J0030+0451	1440.00000000	53098.00000001048646325	0.10000	AXIS
c01_J0030+0451	1440.00000000	53111.99999999118663396	0.10000	AXIS
c01_J0030+0451	1440.00000000	53126.00000002692595302	0.10000	AXIS
c01_J0030+0451	1440.00000000	53139.99999999854099642	0.10000	AXIS
c01_J0030+0451	1440.00000000	53154.00000002016009049	0.10000	AXIS
c01_J0030+0451	1440.00000000	53167.99999997650791883	0.10000	AXIS
c01_J0030+0451	1440.00000000	53181.99999997828629361	0.10000	AXIS
c01_J0030+0451	1440.00000000	53196.00000000686858570	0.10000	AXIS

timing model

Timing model 记录在 Par文件

```
PSRJ            J0030+0451
RAJ              00:30:27.4299630         1   0.00000000083327092134
DECJ            +04:51:39.75230           1   0.00000000193016085164
F0              205.53069608827312545     1   1.6735454617113885805e-13
F1              -4.3060388399134177208e-16 1  2.0847319452591396919e-21
PEPOCH          53000
POSEPOCH        53000
DMEPOCH         53000
PMRA            -4.0541352583640798551    1   0.0600653766421753027O
PMDEC           -5.0337686500180439013    1   0.1400251169870586620 5
PX              4.0229124332613435578     1   0.0206570484239436275 0
EPHVER          5
CLK             UNCORR
MODE 1
EPHEM           DE414
DM              1 1 0
DM1             0 1 0
DM2             0 1 0
```

Right ascension, RA (J2000)
Declination, DEC (J2000)
Proper motion in RA (mas yr^{-1})
Proper motion in DEC (mas yr^{-1})
Spin frequency, f (s^{-1})
$\dot{f}$ (s^{-2})
Parallax, π (mas)
Dispersion measure, DM (cm^{-3} pc)
$\dot{DM}$ (cm^{-3} pc yr^{-1})
$\ddot{DM}$ (cm^{-3} pc yr^{-2})

Binary model
Orbital period, P_b (d)
Epoch of periastron, T_0 (MJD)
Projected semi-major axis, x (lt-s)
Longitude of periastron, ω_0 (deg)
Eccentricity, e
Sine of inclination, $\sin i$
Companion mass, m_c ($M_\odot$)
Derivative of P_b, $\dot{P}_b$
Periastron advance $\dot{\omega}_0$ (deg yr^{-1})
Epoch of ascending node, T_{asc} (MJD)

The pulsar sky location (RAJ and DecJ)， spin frequency and spin-down rate, dispersion measure, proper motion, parallax and (when applicable) binary orbital parameters

Timing residual

Refit TOA with timing model: **Tempo2; PINT**

(TOA - timing model) ~ **residual** ~ (noise + signal)

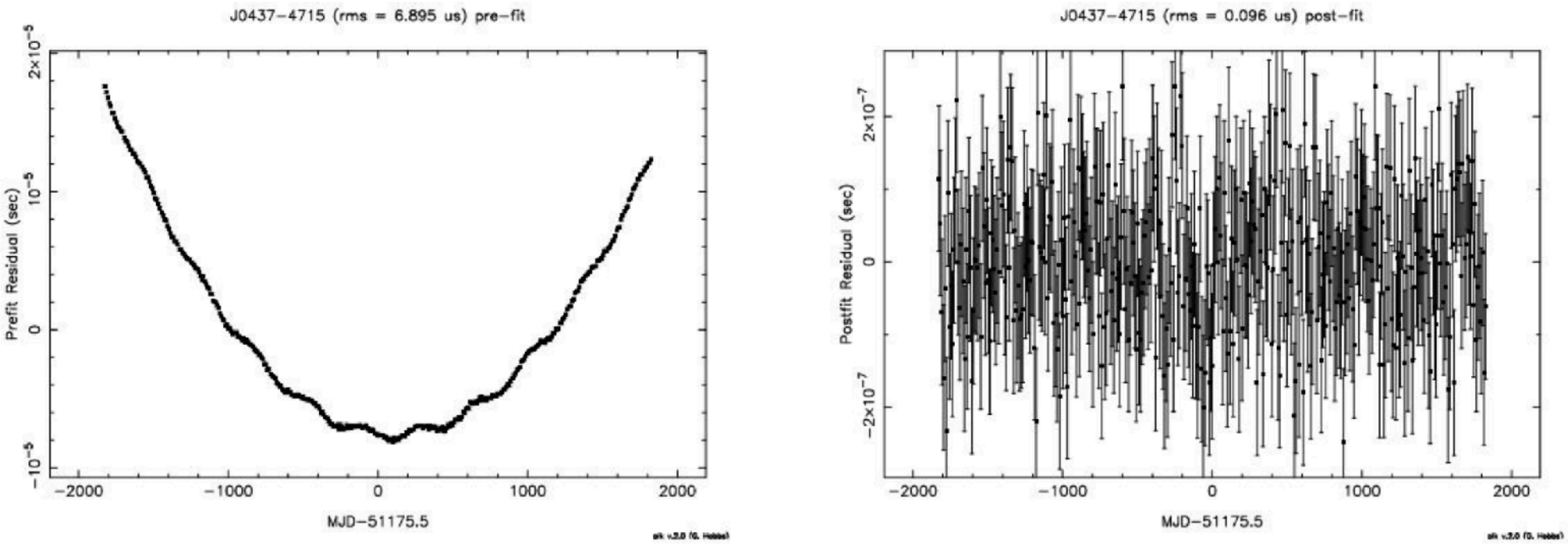

Figure 1: a) pre-fit timing residuals for the test data-set and b) post-fit timing residuals.

Noise

- 按时间的相关性分类：
  1. uncorrelated time (white) noise
  2. time-correlated (red) noise

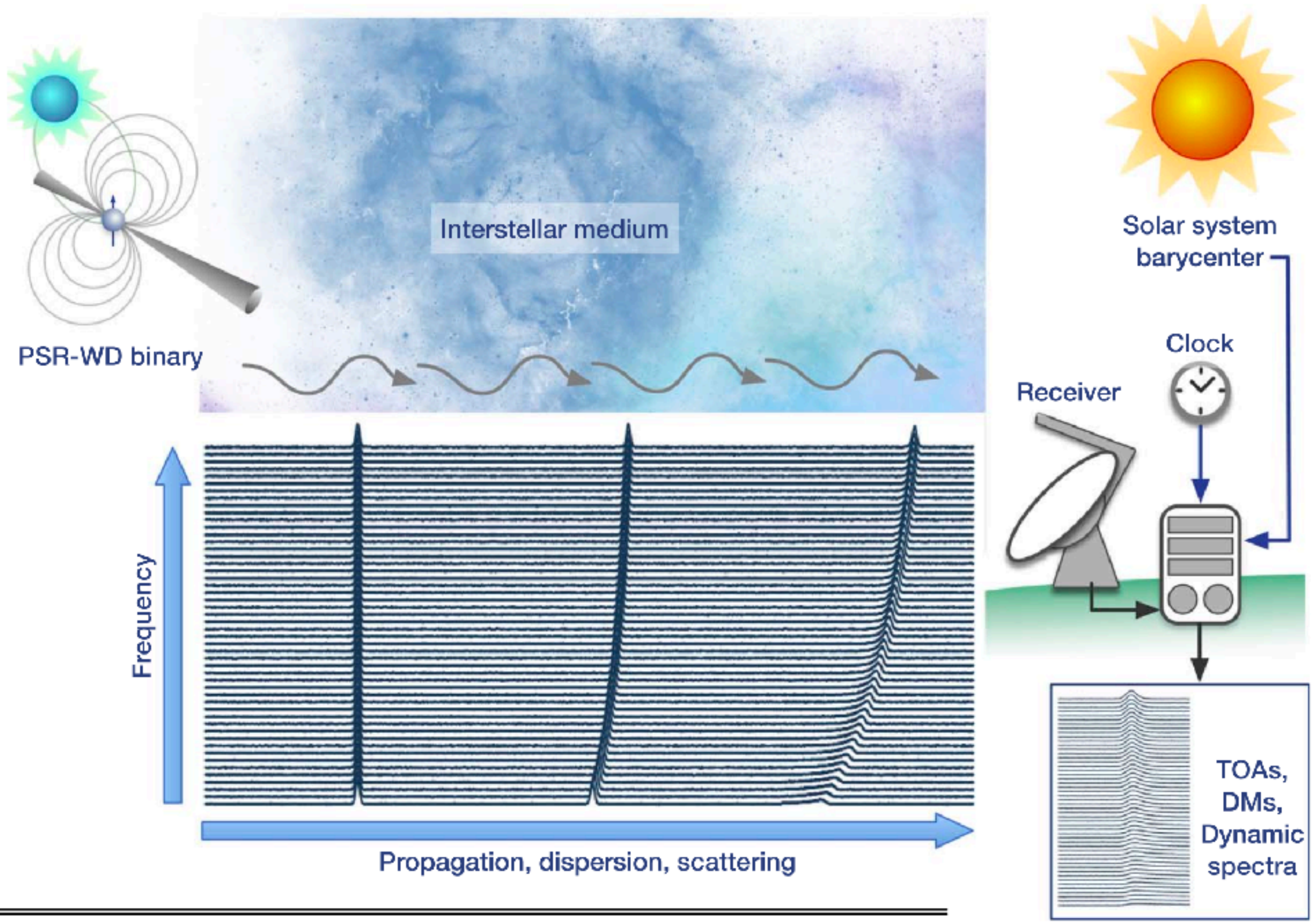

Noise Type	Symbol	Origin	Phenomenological Model Component	Timescale	Spatially Correlated
Radiometer	$\sigma_{S/N}$	Telescope	$\sigma_{S/N}$	Short	
Jitter	σ_J	Pulsar	$\mathcal{J}$	Short	
Diffractive interstellar scintillation	σ_{DISS}	ISM	$\mathcal{Q}$, $\mathcal{J}$	Short	
DM misestimation	δDM	ISM	RN/DMX	Long	
Solar wind DM misestimation	δDM_{sw}	IPM	RN/DMX	Long	✓
Frequency-dependent DM	DM(ν)	ISM	RN/DMX	Long	
RFI		Telescope	$\mathcal{J}$	Short	
Polarization miscalibration		Telescope	$\mathcal{J}$	Both	
Scattering		ISM	$\mathcal{F}$, $\mathcal{J}$	Short	
Solar system barycenter mismodeling		solar system	RN	Long	✓
Clock errors		Telescope	RN	Long	✓

White noise

the data. These three WN terms—EFAC ($\mathcal{F}$), EQUAD ($\mathcal{Q}$), and ECORR ($\mathcal{J}$)—come together with receiver/back-end combination re/be dependence as

$$C_{ij} = \mathcal{F}^2(re/be)[\sigma^2_{\mathrm{S/N},i} + \mathcal{Q}^2(re/be)]\,\delta_{ij} + \mathcal{J}^2(re/be)\,\mathcal{U}_{ij}, \tag{2}$$

where the i, j denote TOA indices across all observing epochs, δ_{ij} is the Kronecker delta, and we omit the dependence on receiver and back end, re/be, from here on for simplicity.

```
J0023+0923_430_ASP_efac
J0023+0923_430_ASP_log10_ecorr
J0023+0923_430_ASP_log10_equad
J0023+0923_430_PUPPI_efac
J0023+0923_430_PUPPI_log10_ecorr
J0023+0923_430_PUPPI_log10_equad
J0023+0923_L-wide_ASP_efac
J0023+0923_L-wide_ASP_log10_ecorr
J0023+0923_L-wide_ASP_log10_equad
J0023+0923_L-wide_PUPPI_efac
J0023+0923_L-wide_PUPPI_log10_ecorr
J0023+0923_L-wide_PUPPI_log10_equad
```

参数个数： 3 per puslar/re/be

NanoGrav (15yr) 中一共是有700多个白噪声参数

$$C^{\mathrm{epoch}} = \begin{bmatrix} \mathcal{F}^2[\sigma^2_{\mathrm{S/N}}(\nu_1) + \mathcal{Q}^2] + \mathcal{J}^2 & \mathcal{J}^2 & \cdots & \mathcal{J}^2 \\ \mathcal{J}^2 & \mathcal{F}^2[\sigma^2_{\mathrm{S/N}}(\nu_2) + \mathcal{Q}^2] + \mathcal{J}^2 & \cdots & \mathcal{J}^2 \\ \vdots & \vdots & \ddots & \vdots \\ \mathcal{J}^2 & \mathcal{J}^2 & \cdots & \mathcal{F}^2[\sigma^2_{\mathrm{S/N}}(\nu_N) + \mathcal{Q}^2] + \mathcal{J}^2 \end{bmatrix},$$

Red noise

- Red noise power spectra are modeled with a power law

$$S_{RN} = \frac{A^2}{12\pi^2}\left(\frac{f}{1\mathrm{yr}}\right)^{-\gamma}\frac{\mathrm{yr}^3}{T},$$

- 可以按 radio frequency（v） 的相关性在细分成

1. Achromatic (spin noise).　　　2. chromatic (DM noise; Scatter noise)

$$y(t) = \sum_{j=1}^{N_{\mathrm{coef}}} Y_j \left(a_j \cos(j\omega t) + b_j \sin(j\omega t)\right)\left(\frac{\nu}{\nu_{\mathrm{ref}}}\right)^{-\alpha},\qquad Y_j = \sqrt{\frac{A^2}{K_{\mathrm{scale}}}\frac{s_{\mathrm{yr}}{}^3}{T_{\mathrm{span}}}\left(\frac{f_j}{f_{\mathrm{yr}}}\right)^{-\gamma}},$$

(spin)

Parameter	Red	DM	Scatter
K_{scale}	$12\pi^2$	k_{DM}^2	$12\pi^2$
α	0	2	4
Prior($\log_{10}(A)$)	$\mathcal{U}(-18,-10)$	$\mathcal{U}(-18,-10)$	$\mathcal{U}(-18,-10)$
Prior(γ)	$\mathcal{U}(0,7)$	$\mathcal{U}(0,7)$	$\mathcal{U}(0,7)$

主要是pulsar和星际介质ISM导致，每个pulsar都有一组自己的红噪声，彼此独立

Other noise

Dip noise

由于视线方向上出现**高密度的等离子体团**,

引入**额外的noise**

$$d_{\exp}(t_i, \nu_k\, ; \theta_{\exp}) = A \left(\frac{\nu_k}{\nu_{\rm ref}}\right)^{-\alpha} \exp\left(-\frac{t_i - t_0}{\tau}\right),$$

PSR J1603–7202 and PSR J1713+0747

Table 2. Parameter priors for the two exponential dips included in the noise models for PSR J1713+0747.

Parameter	Prior
A [s]	$\log_{10}\mathcal{U}(10^{-10}, 10^{-2})$
τ [day]	$\log_{10}\mathcal{U}(1, 10^{2.5})$
t_0 (1st event) [MJD]	$\mathcal{U}(54650, 54850)$
t_0 (2nd event) [MJD]	$\mathcal{U}(57490, 57530)$
α (1st event)	4 (fixed value)
α (2nd event)	1 (fixed value)

Solar System Ephemeris noise

BayesEphem parameters ($\psi^{\rm sys}$)			
$z_{\rm drift}$	Drift-rate of Earth's orbit about ecliptic z-axis	U$[-10^{-9}, 10^{-9}]$ rad yr^{-1}	one parameter per PTA
$\Delta M_{\rm jupiter}$	Perturbation of Jupiter's mass	$\mathcal{N}(0, 1.5 \times 10^{-11}) M_\odot$	one parameter per PTA
$\Delta M_{\rm saturn}$	Perturbation of Saturn's mass	$\mathcal{N}(0, 8.2 \times 10^{-12}) M_\odot$	one parameter per PTA
$\Delta M_{\rm uranus}$	Perturbation of Uranus' mass	$\mathcal{N}(0, 5.7 \times 10^{-11}) M_\odot$	one parameter per PTA
$\Delta M_{\rm neptune}$	Perturbation of Neptune's mass	$\mathcal{N}(0, 7.9 \times 10^{-11}) M_\odot$	one parameter per PTA
PCA_i	Principal components of Jupiter's orbit	U$[-0.05, 0.05]$	six parameters per PTA

The orbital periods of the giant planets range from 11.9 to 164.8yr, corresponding to frequencies of ~0.4–2.7 nHz, similar to the GWB frequency range that is probed by PTAs.

Noise in Radio PTA vs Gamma-ray PTA

对比Radio PTA，

优点：Gamma-ray PTA 的噪声要干净很多，不受色散的影响。

缺点：统计量小

Table S1: **Sources of noise in radio and gamma-ray pulsar timing array data.** The list is incomplete and qualitative: for each noise source, we attempt to give an estimate of the importance (amplitude in residuals, or difficulty of complete mitigation) and complexity (degrees of freedom (d.o.f.) in existing models for a typical pulsar). Dashes indicate that the entry is not applicable, and a question mark that its impact is unknown.

	Radio		Gamma ray		
Noise Source	Impact	d.o.f.	Impact	d.o.f.	Note
White Noise					
Measurement	moderate	–	major	–	Sensitivity is major limiting factor for gamma rays.
RFI	minor	?	–	–	RFI varies widely between observing systems.
Calibration	minor	?	–	–	Affects certain pulsars/observing systems.
Jitter	moderate	10s	–	–	Jitter affects high signal-to-noise observations.
Red Noise					
DM variation	major	100s	–	–	DM(t) drives radio PTA observing strategies.
Solar wind	moderate	∼10s	–	–	Solar wind mitigation is poorly supported.
Scattering	moderate	100s	–	–	Affects some pulsars/low radio frequencies.
Pulse variability	moderate	0–10s	–	?	No gamma-ray MSP pulse profile changes known.
Discontinuities	moderate	10s	–	–	LAT data are continuous, not a general property.
Spin noise	major	10s–100s	major	10s	Fewer d.o.f. needed for less precise LAT data.

https://www.science.org/doi/10.1126/science.abm3231

Outline

1. 脉冲星计时阵列简介

2. TOA数据及噪声模型

3.超轻暗物质间接探测

Ultralight Dark Matter

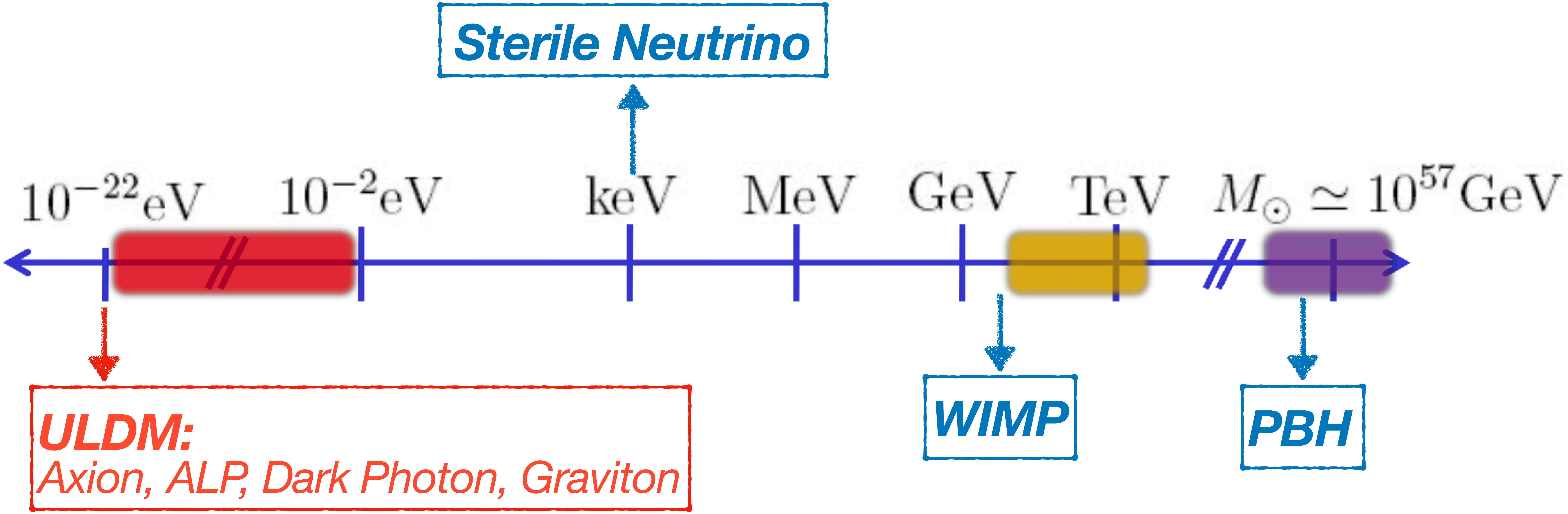

- Have an advantage in forecasting small-scale structures.
  (“core-cusp problem” and “missing-satellite problem”)

- Hard to detect with common particle detectors.

Our work on Dark matter

Ultralight Dark matter appear like a coherent wave with wavelength comparable to a dwarf galaxy. Both the pulsar and the earth would **oscillate in the ultralight Dark matter background**, **resulting in time residuals of pulses.**

$$\delta \boldsymbol{x}_{e,p}(t) \simeq -\frac{\epsilon e q}{m_A m} \boldsymbol{A_0}^{e,p} \cos\left[m_A(t-t_0)+\alpha_{e,p}\right]$$

$$\Delta t_r^d(t) = \frac{\left|\boldsymbol{d} + \delta\boldsymbol{x}_p\left(t - \frac{|\boldsymbol{d}|}{v(t)}\right) - \delta\boldsymbol{x}_e(t)\right| - |\boldsymbol{d}|}{v(t)} \simeq \frac{\boldsymbol{n}_p \cdot \Delta \boldsymbol{x}(t)}{v(t)},$$

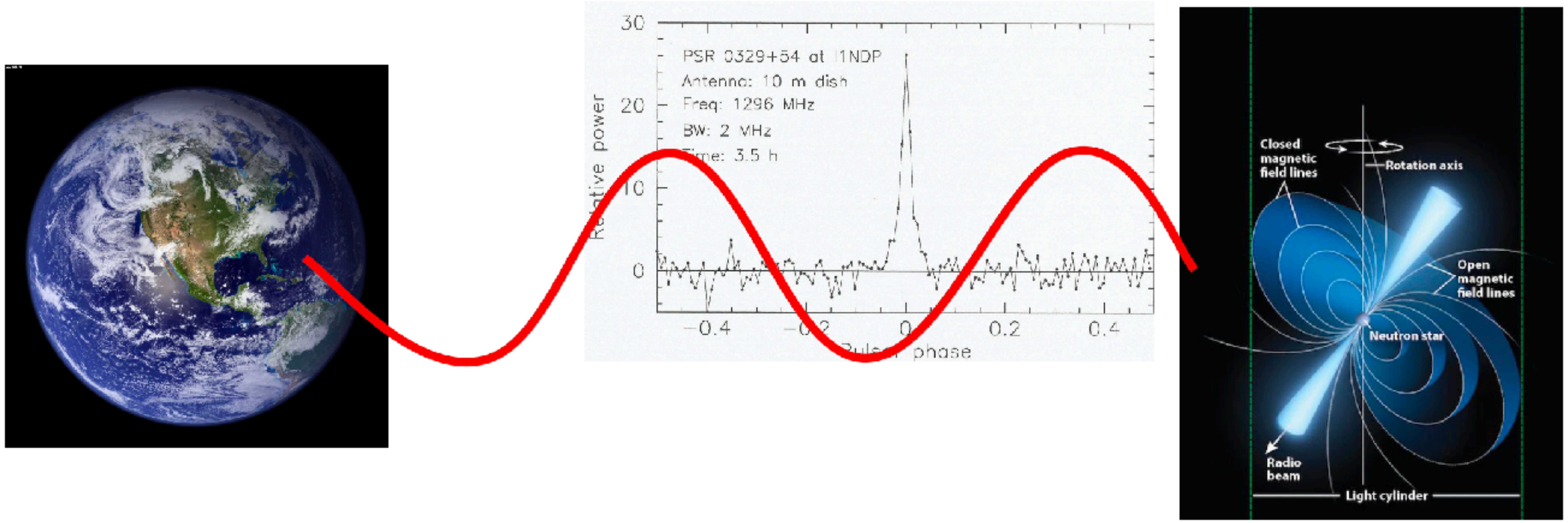

Our work on Dark matter

- Coherence length: 0.4 $(m/10^{-22}eV)^{-1}$ kpc
- Frequency: 30 nHz×$(m/10^{-22}eV)$
- Suitable for PTA observations with ~10-year timescales

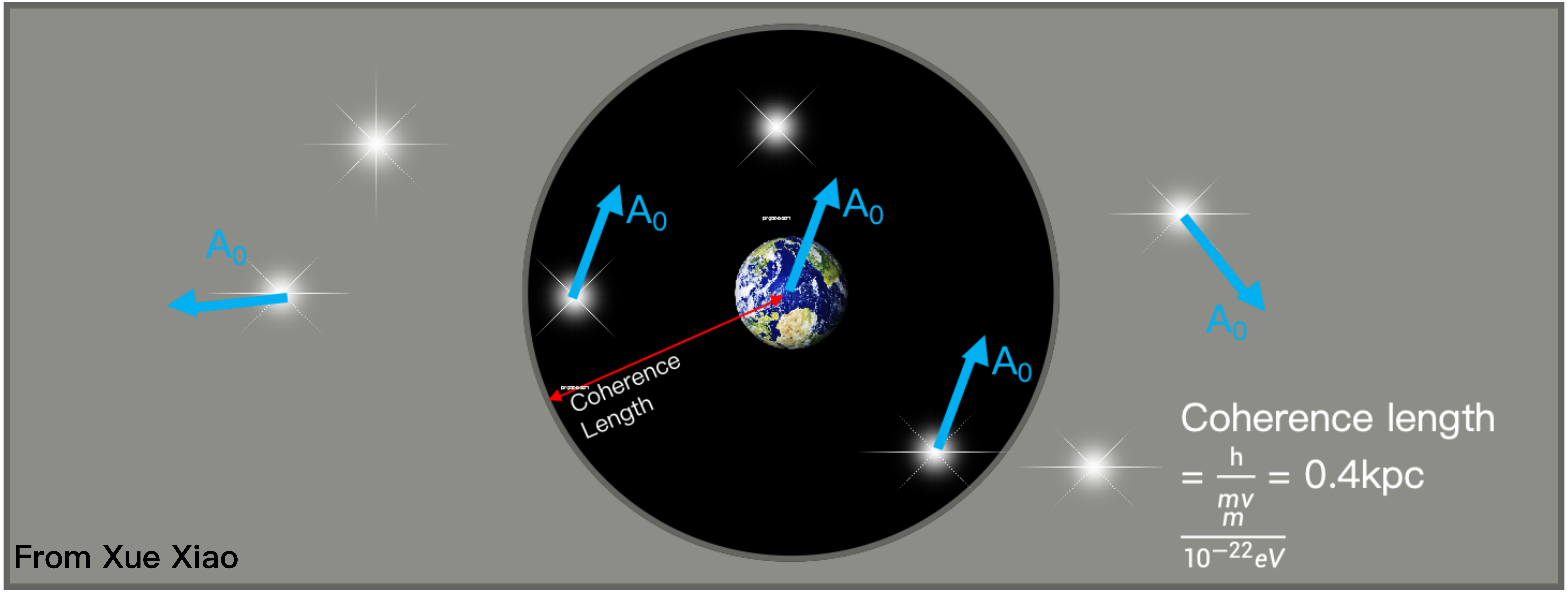

Our work on Dark matter (1)

1. 利用**PPTA**数据搜寻**超轻暗光子 dark photon**的信号。

超轻暗光子的第五种力就会导致同样位于银河系中的**地球和脉冲星发生震荡**，从而导致脉冲星电磁**脉冲到达时间的周期性变化**。

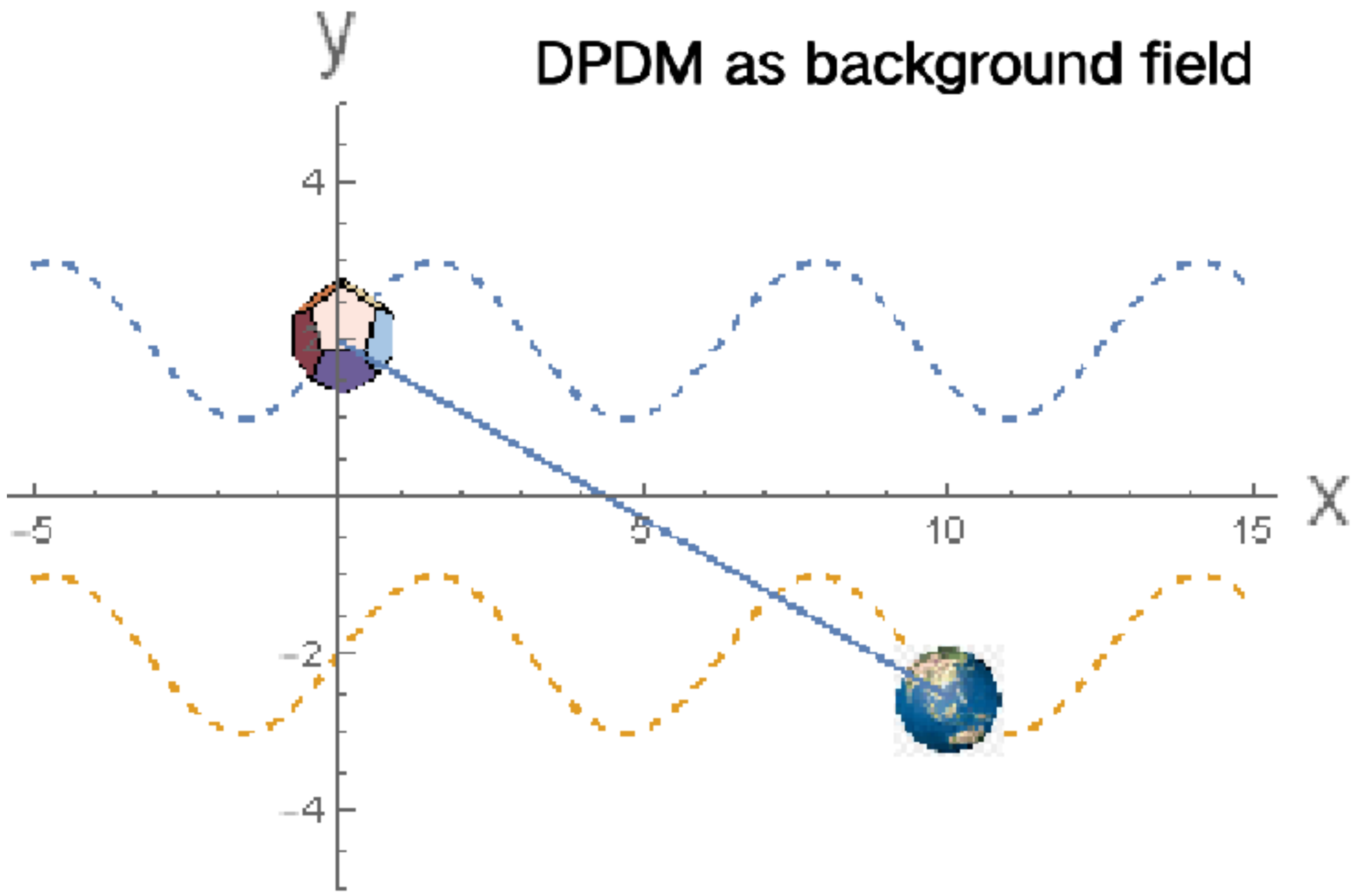

PHYSICAL REVIEW RESEARCH **4**, L012022 (2022)

Letter | Editors' Suggestion

High-precision search for dark photon dark matter with the Parkes Pulsar Timing Array

Xiao Xue,[1] Zi-Qing Xia,[2] Xingjiang Zhu,[3,4,5] Yue Zhao,[6] Jing Shu,[7,8,9,10,11,12,*] Qiang Yuan,[2,10,13,†] N. D. Ramesh Bhat,[14] Andrew D. Cameron,[5,15,16] Shi Dai,[17,15] Yi Feng,[18] Boris Goncharov,[4,5] George Hobbs,[15] Eric Howard,[15,19] Richard N. Manchester,[15] Aditya Parthasarathy,[16,20] Daniel J. Reardon,[5,16] Christopher J. Russell,[21] Ryan M. Shannon,[5,16] Renée Spiewak,[16,22] Nithyanandan Thyagarajan,[23] Jingbo Wang,[24] Lei Zhang,[25] and Songbo Zhang[26]
(PPTA Collaboration)

（和PPTA合作组合作完成，发表于PHYS. REV. R, 2022 Editors' Suggestion）

Our work on Dark matter (1)

PPTA DR2

26 MSPs; 15yr

计时精度：百纳秒

Pulsar Name	$N_{\rm obs}$	σ (μs)	$T_{\rm obs}$ (year)	D (kpc)
J0437−4715	29262	0.29	15.03[a]	0.16
J0613−0200	5920	2.50	14.20	0.78
J0711−6830	5547	6.20	14.21	0.11
J1017−7156	4053	1.58	7.77	0.26
J1022+1001	7656	5.51	14.20	0.72
J1024−0719	2643	4.36	14.09	1.22
J1045−4509	5611	9.18	14.15	0.34
J1125−6014	1407	1.98	12.34	0.99
J1446−4701	508	2.20	7.36	1.57
J1545−4550	1634	2.25	6.97	2.25
J1600−3053	7047	2.22	14.21	2.0
J1603−7202	5347	4.95	14.21	0.53
J1643−1224	5941	4.04	14.21	0.74
J1713+0747	7804	1.60	14.21	1.22
J1730−2304	4549	5.66	14.21	0.62
J1732−5049	807	7.03	7.23	1.87
J1744−1134	6717	2.25	14.21	0.4
J1824−2452A	2626	2.19	13.80	5.50
J1832−0836	326	1.43	5.4	2.5
J1857+0943	3840	5.56	14.21	1.2
J1909−3744	14627	0.67	14.21	1.14
J1939+2134	4941	0.47	14.09	3.5
J2124−3358	4941	8.86	14.21	0.41
J2129−5721	2879	3.50	13.88	3.20
J2145−0750	6867	5.09	14.09	0.61
J2241−5236	5224	0.83	8.2	0.75

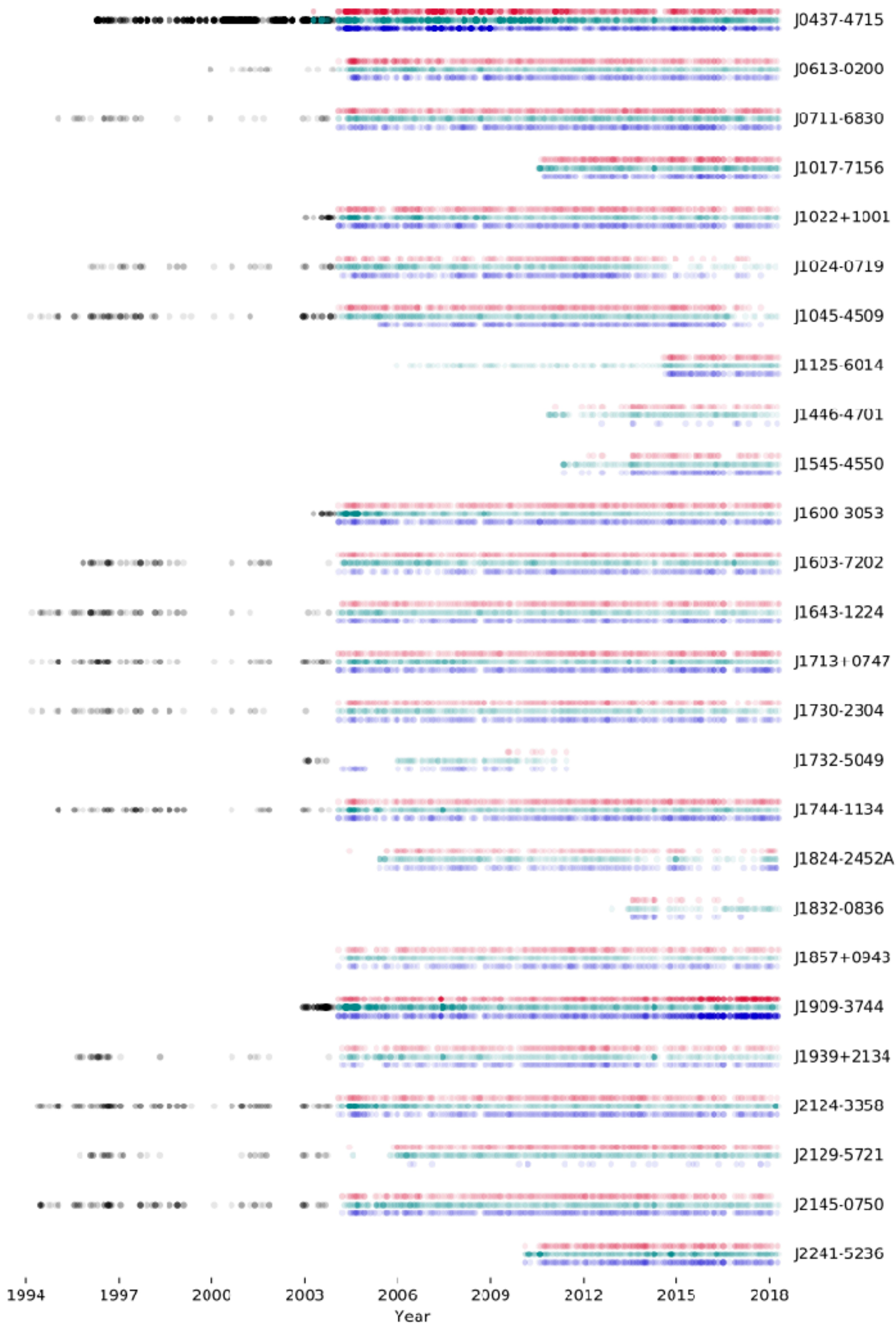

Our work on Dark matter (1)

在搜寻暗物质的过程中发现的疑似信号，其的频率与水星的周期相近

疑似信号参数

TABLE S3: The best-fit dark photon parameters that favor the $\mathcal{H}_1$ hypothesis with a total of 26 pulsars.

Interaction	m_A(eV)	f(Hz)	ϵ	λ_{LR}^{max}
$U(1)_B$	$10^{-21.37}$	1.02×10^{-7}	$10^{-22.68}$	472
$U(1)_{B-L}$	$10^{-21.37}$	1.02×10^{-7}	$10^{-22.87}$	498

噪声和信号参数

	Parameter	Prior	Description
White Noise ϑ_W	EFAC	U[0.01,10]	one per backend
	EQUAD	log-U $[10^{-10},10^{-4}]$	one per backend
Spin Noise ϑ_{SN}	γ_{SN}	U[0,7]	one per pulsar
	A_{SN}	log-U$[10^{-21},10^{-9}]$	one per pulsar
DM Noise ϑ_{DM}	γ_{DM}	U[0,7]	one per pulsar
	A_{DM}	log-U$[10^{-21},10^{-9}]$	one per pulsar
Band Noise ϑ_{BN} for J0437 and J1939	γ_{BN}	U[0,7]	one per band
	A_{BN}	log-U$[10^{-21},10^{-9}]$	one per band
Dark photon Parameters ϑ_{DPDM}	α_p	U$[0,2\pi]$	one per pulsar
	α_e^i	U$[0,2\pi]$	three per PTA
	$(\tilde{A}_0^p)^2$	$f(x)=e^{-x}$	one per pulsar*
	$(\tilde{A}_0^{e,i})^2$	$f(x)=e^{-x}$	three per PTA
	ϵ	log-U$[10^{-28},10^{-16}]$	one per PTA
	m_A	log-U$[10^{-23.5},10^{-21}]$	one per PTA
BayesEphem Parameters ϑ_{BE}	z_{drift}	U$[-10^{-9},10^{-9}]$	one per PTA
	$\Delta M_{Jupiter}$	N$(0, 1.5\times10^{-11})$	one per PTA
	ΔM_{Saturn}	N$(0, 8.2\times10^{-12})$	one per PTA
	ΔM_{Uranus}	N$(0, 5.7\times10^{-11})$	one per PTA
	$\Delta M_{Neptune}$	N$(0, 7.9\times10^{-11})$	one per PTA
	PCA_i	U[−0.05,0.05]	six per PTA

Our work on Dark matter (1)

对超轻暗光子（<1e-22eV）给出了**国际上最强的限制结果，比目前最好的实验室探测试验要强3个数量级。**

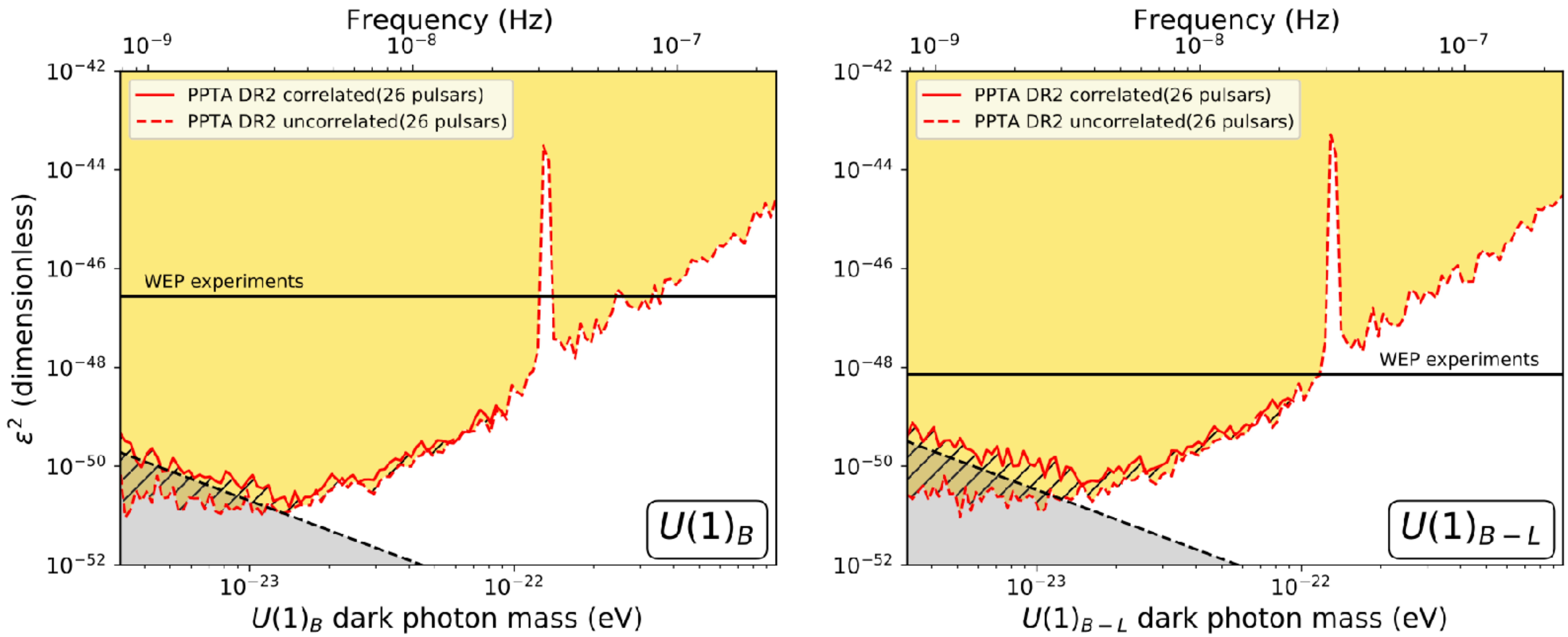

Our work on Dark matter (2)

2. 利用Fermi-LAT(Gamma-ray) PTA 搜寻多种超轻暗物质粒子。

4种超轻暗物质的PTA可探测效应

1.自旋为0超轻暗物质的引力效应

2. 自旋为1超轻暗物质的引力效应

3. 超轻暗光子的第五种力效应

4. 自旋为2超轻暗物质的修改引力效应

Fermi-LAT PTA:

- Gamma-ray
- 12.5 yr
- 29 MSPs
- 精度~微秒
- 1 TOA per 0.5 yr
- No DM noise

PHYSICAL REVIEW D **107,** L121302 (2023)

Letter

发表于PRD Letter (2023)

Constraining ultralight dark matter using the Fermi-LAT pulsar timing array

Zi-Qing Xia,[1] Tian-Peng Tang,[1,2] Xiaoyuan Huang,[1,2,*] Qiang Yuan,[1,2,†] and Yi-Zhong Fan[1,2,‡]

[1]*Key Laboratory of DM and Space Astronomy, Purple Mountain Observatory, Chinese Academy of Sciences, Nanjing 210033, China*

[2]*School of Astronomy and Space Science, University of Science and Technology of China, Hefei, Anhui 230026, China*

(Received 11 April 2023; accepted 22 May 2023; published 28 June 2023)

Our work on Dark matter (2)

The parameters of signal and noise models

Model	Parameter	Prior	Description
Spin-0: Gravitational Signal	θ_p	U[0,2π]	Phase for the pulsar term, one per pulsar
	θ_e	U[0,2π]	Phase for the Earth term, one per PTA
	Ψ	log-U[10^{-20},10^{-12}]	Oscillation amplitude for the Spin-0 ULDM field, one per PTA
	m	log-U[10^{-24},10^{-21}]	Mass for the Spin-0 ULDM, one per PTA
Spin-1: Gravitational Signal	θ_p	U[0,2π]	Phase for the pulsar term, one per pulsar
	θ_e	U[0,2π]	Phase for the Earth term, one per PTA
	$\theta_{\rm osc}$	U[0,π]	Polar angle of the Spin-1 ULDM oscillation direction, one per PTA
	$\phi_{\rm osc}$	U[0,2π]	Azimuth angle of the Spin-1 ULDM oscillation direction, one per PTA
	$h_{\rm osc}$	log-U[10^{-19},10^{-9}]	Oscillation amplitude for the Spin-1 ULDM field, one per PTA
	m	log-U[10^{-24},10^{-21}]	Mass for the Spin-0 ULDM, one per PTA
Spin-1: Fifth-Force Signal	θ_p	U[0,2π]	Phase for the pulsar term, one per pulsar
	θ_e^i	U[0,2π]	Phase for the Earth term, three per PTA
	$(\tilde{A}_0^i)^2$	$f(x) = e^{-x}$	Normalized gauge potential of the Dark Photon field, three per PTA
	ϵ	log-U[10^{-28},10^{-16}]	Coupling strength for the Dark Photon field, one per PTA
	m	log-U[10^{-24},10^{-21}]	Mass for the Dark Photon, one per PTA
Spin-2: Modified Gravitational Signal	θ_p	U[0,2π]	Phase for the pulsar term, one per pulsar
	θ_e	U[0,2π]	Phase for the Earth term, one per PTA
	α	log-U[10^{-12},10^{-1}]	Coupling strength for the Spin-2 ULDM field, one per PTA
	m	log-U[10^{-24},10^{-21}]	Mass for the Spin-2 ULDM, one per PTA
White Noise (WN)	EFAC	U[0.1,5]	Re-scaling factor, one per pulsar
	EQUAD	log-U [10^{-9},10^{-5}]	Extra white noise, one per pulsar
Red Noise (RN)	A	log-U[10^{-18},10^{-9}]	Amplitude for red noise, one per pulsar
	γ	U[0,7]	Index for red noise, one per pulsar
BayesEphem Noise (BEph)	$z_{\rm drift}$	U[-10^{-9},10^{-9}]	Drift-rate of Earth's orbit about ecliptic z-axis,one per PTA
	$\Delta M_{\rm Jupiter}$	N(0, 1.5×10^{-11})	Perturbation of Jupiter's mass, one per PTA
	$\Delta M_{\rm Saturn}$	N(0, 8.2×10^{-12})	Perturbation of Saturn's mass, one per PTA
	$\Delta M_{\rm Uranus}$	N(0, 5.7×10^{-11})	Perturbation of Uranus' mass, one per PTA
	$\Delta M_{\rm Neptune}$	N(0, 7.9×10^{-11})	Perturbation of Neptune's mass, one per PTA
	PCA$_i$	U[-0.05,0.05]	Principal components of Jupiter's orbit, six per PTA

- **No significant signals** of ULDM are found in the Fermi-LAT PTA.

Our work on Dark matter (2)

限制情况

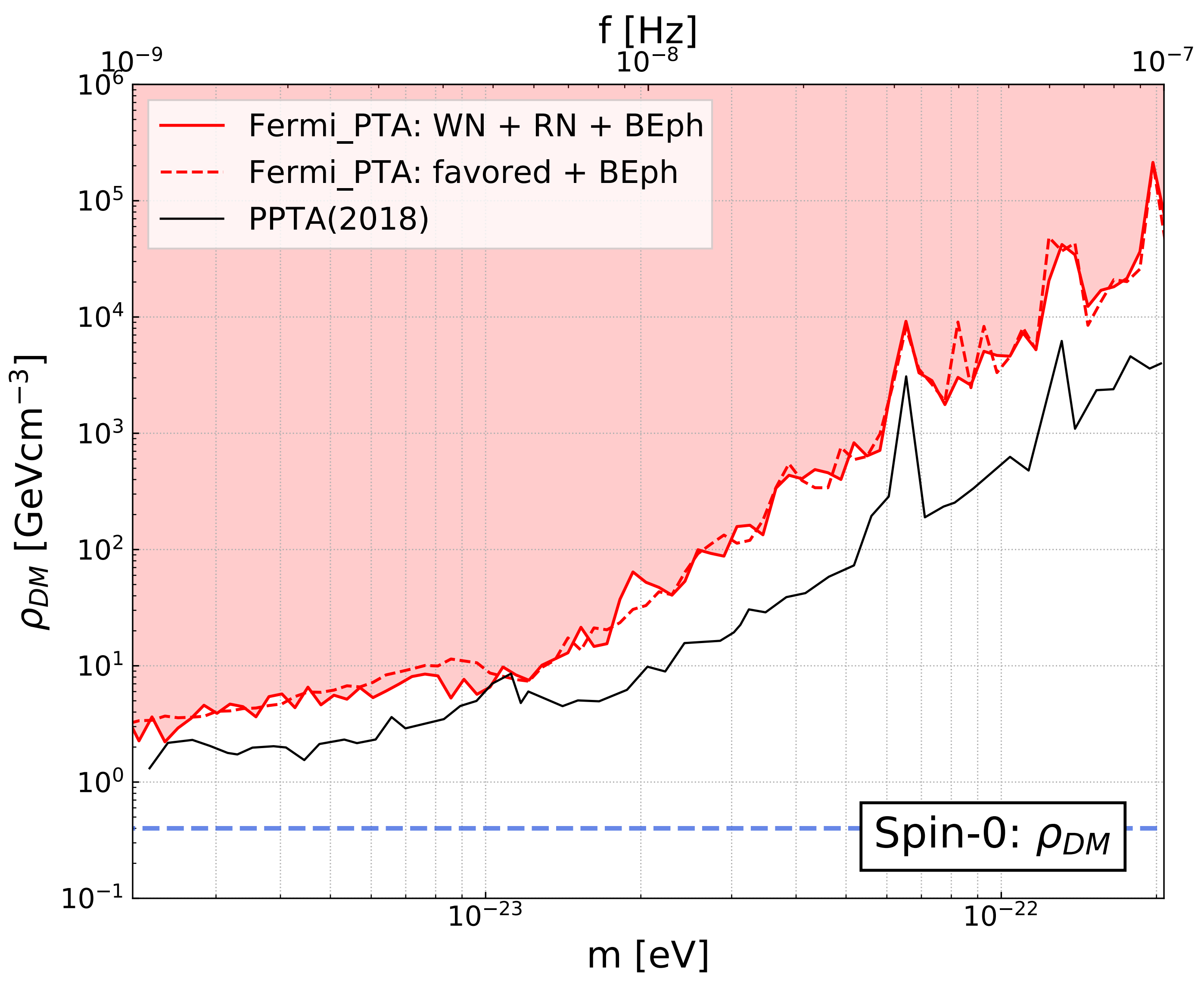

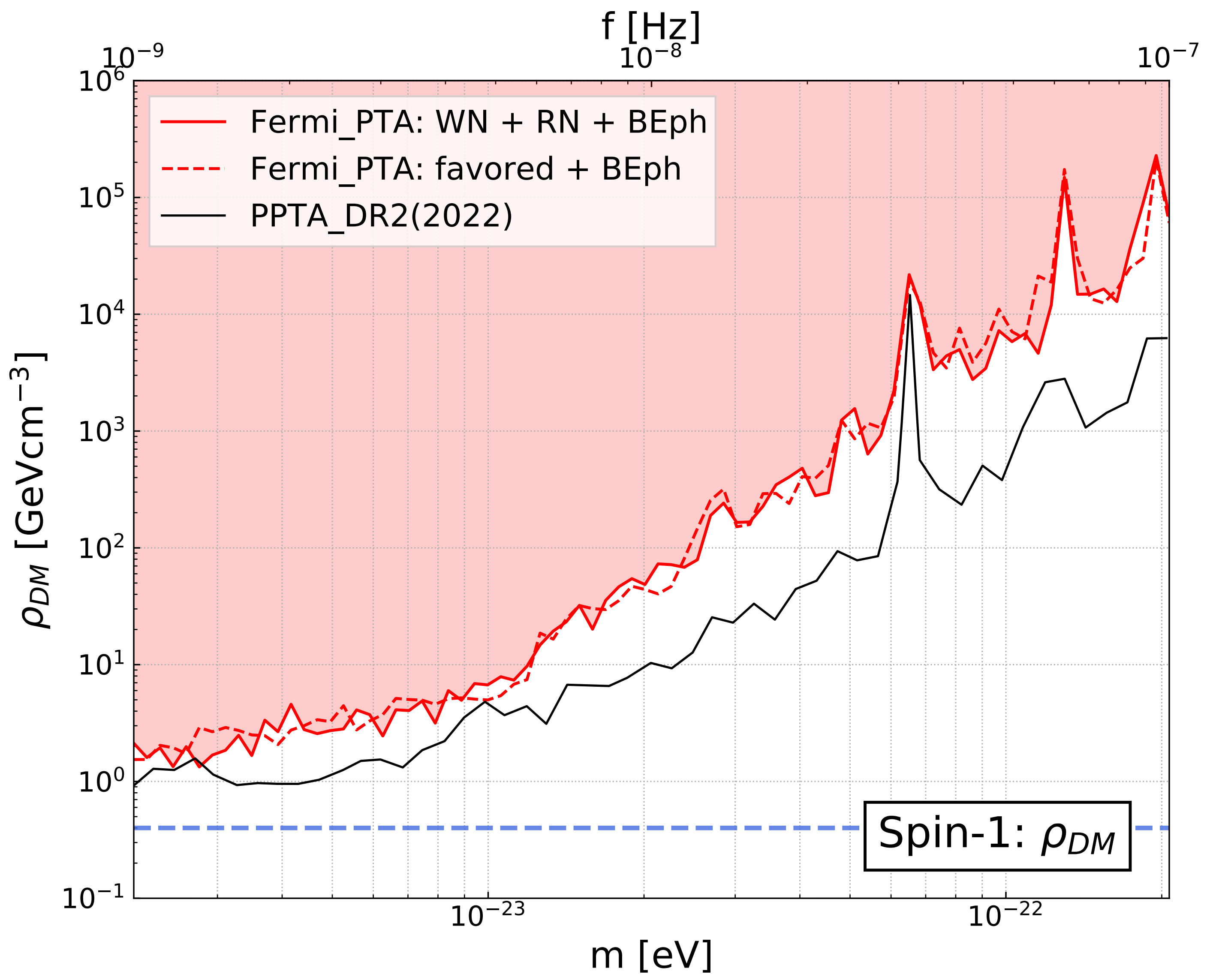

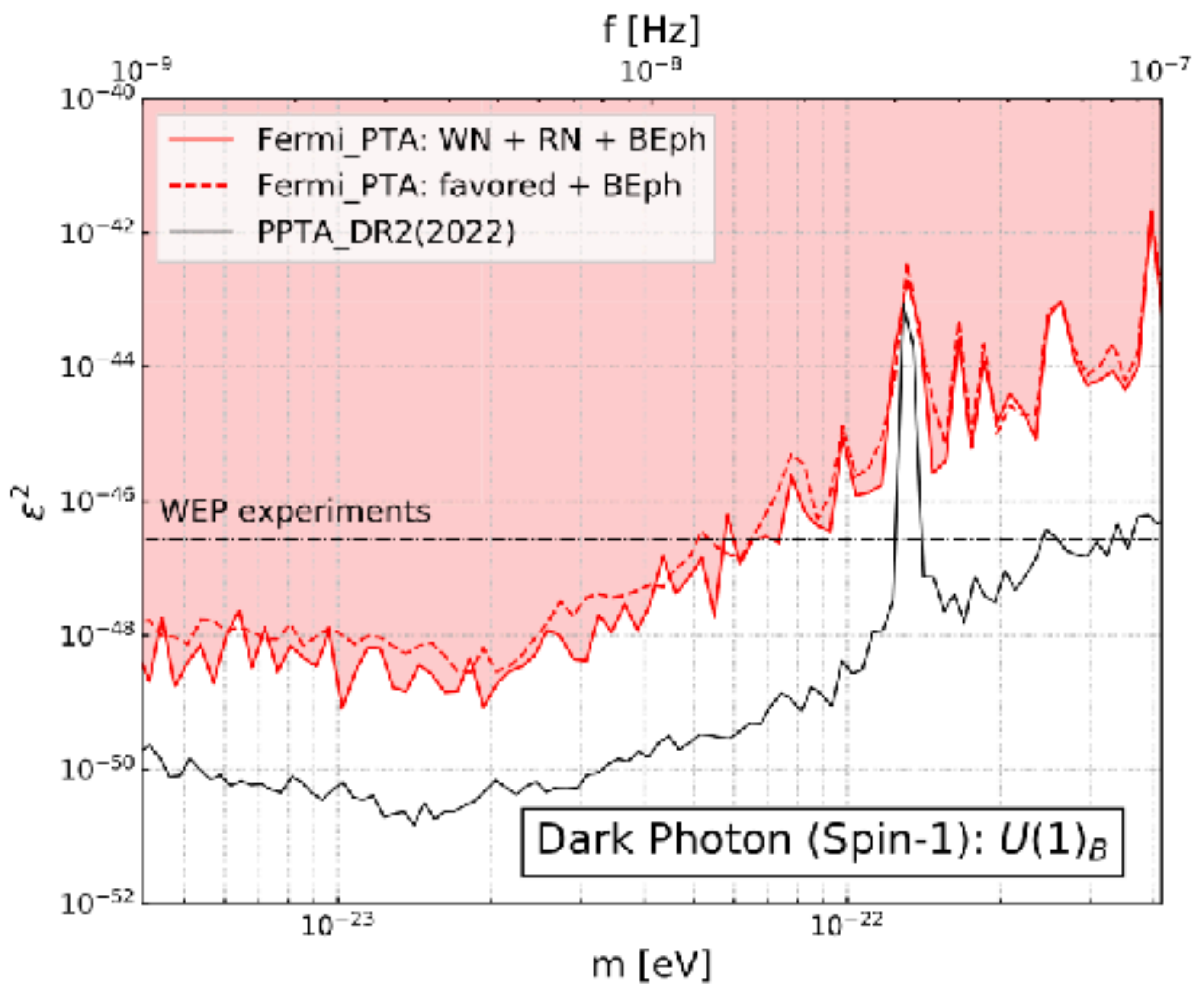

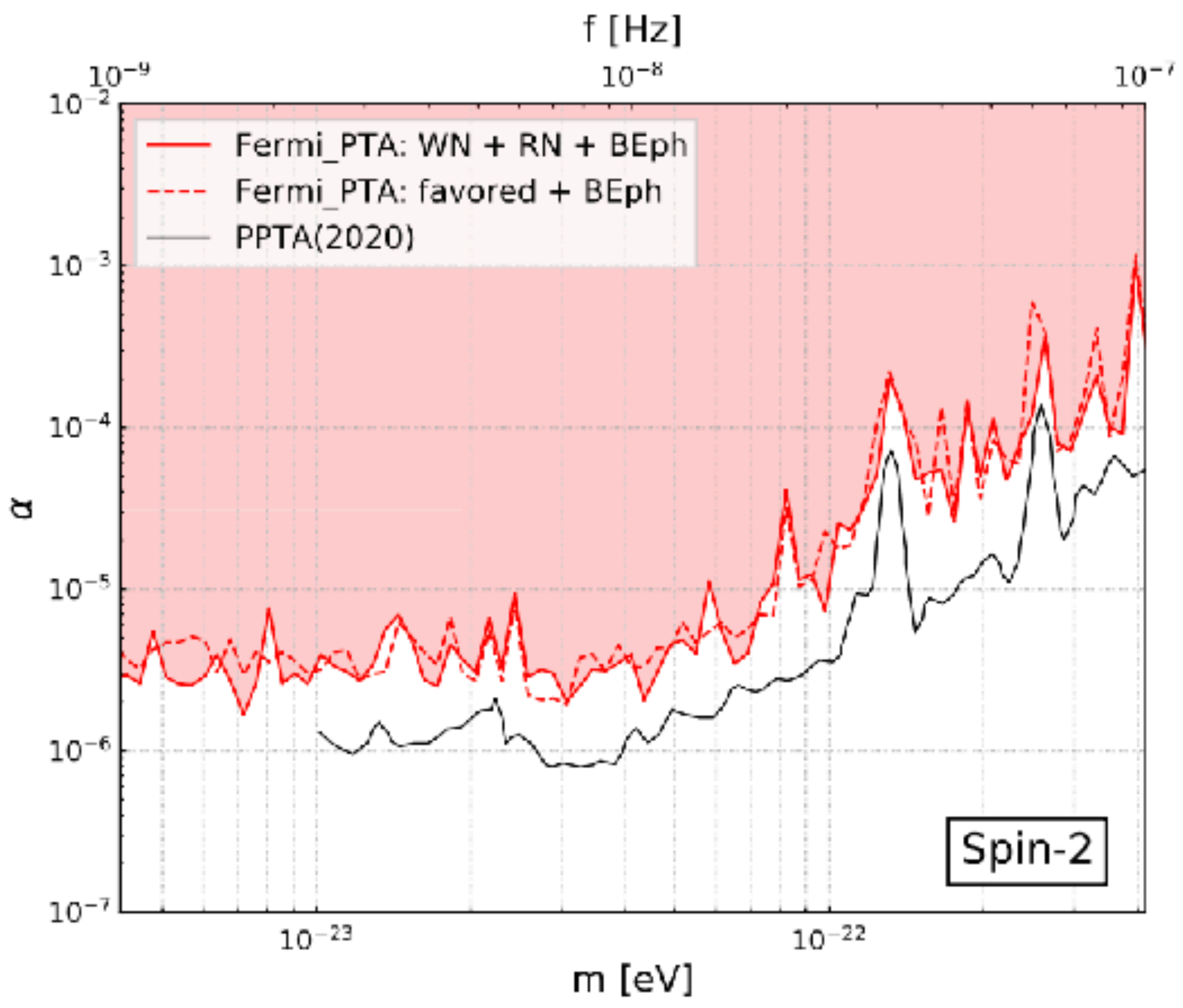

未来 - Very Large Area gamma-ray Space Telescope (VLAST)

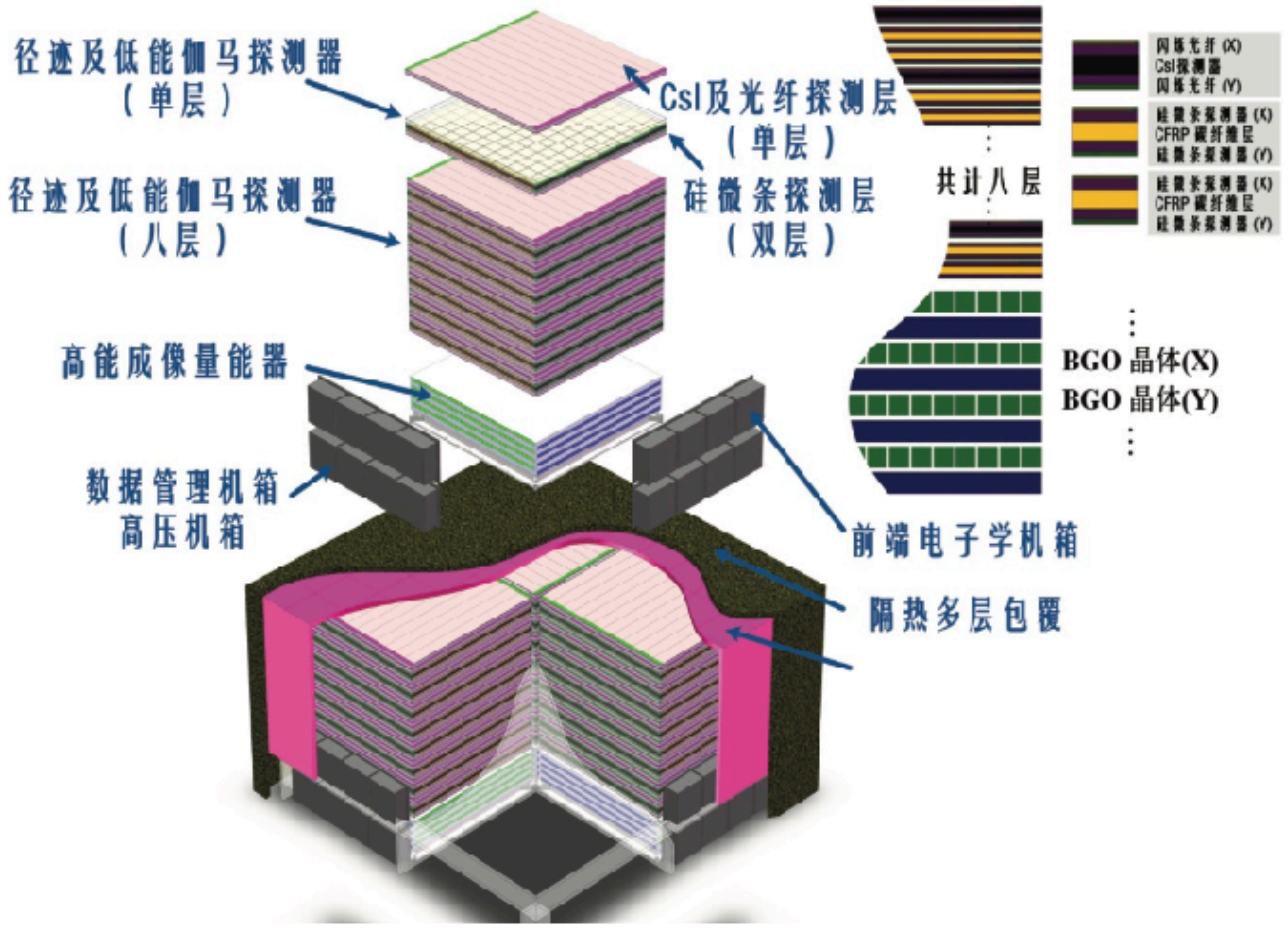

第 63 卷 第 3 期 天 文 学 报 Vol. 63 No. 3
2022 年 5 月 ACTA ASTRONOMICA SINICA May, 2022

doi: 10.15940/j.cnki.0001-5245.2022.03.002

甚大面积伽马射线空间望远镜计划*

范一中[1,2,3†] 常 进[1,2,3,8†] 郭建华[1,2,3] 袁 强[1,2,3] 胡一鸣[1,2] 李 翔[1,2,3]
岳 川[1,2] 黄光顺[4,5] 刘树彬[4,5] 封常青[4,5] 张云龙[4,5] 魏逸丰[4,5]

Improve by a factor of ~10 than Fermi-LAT

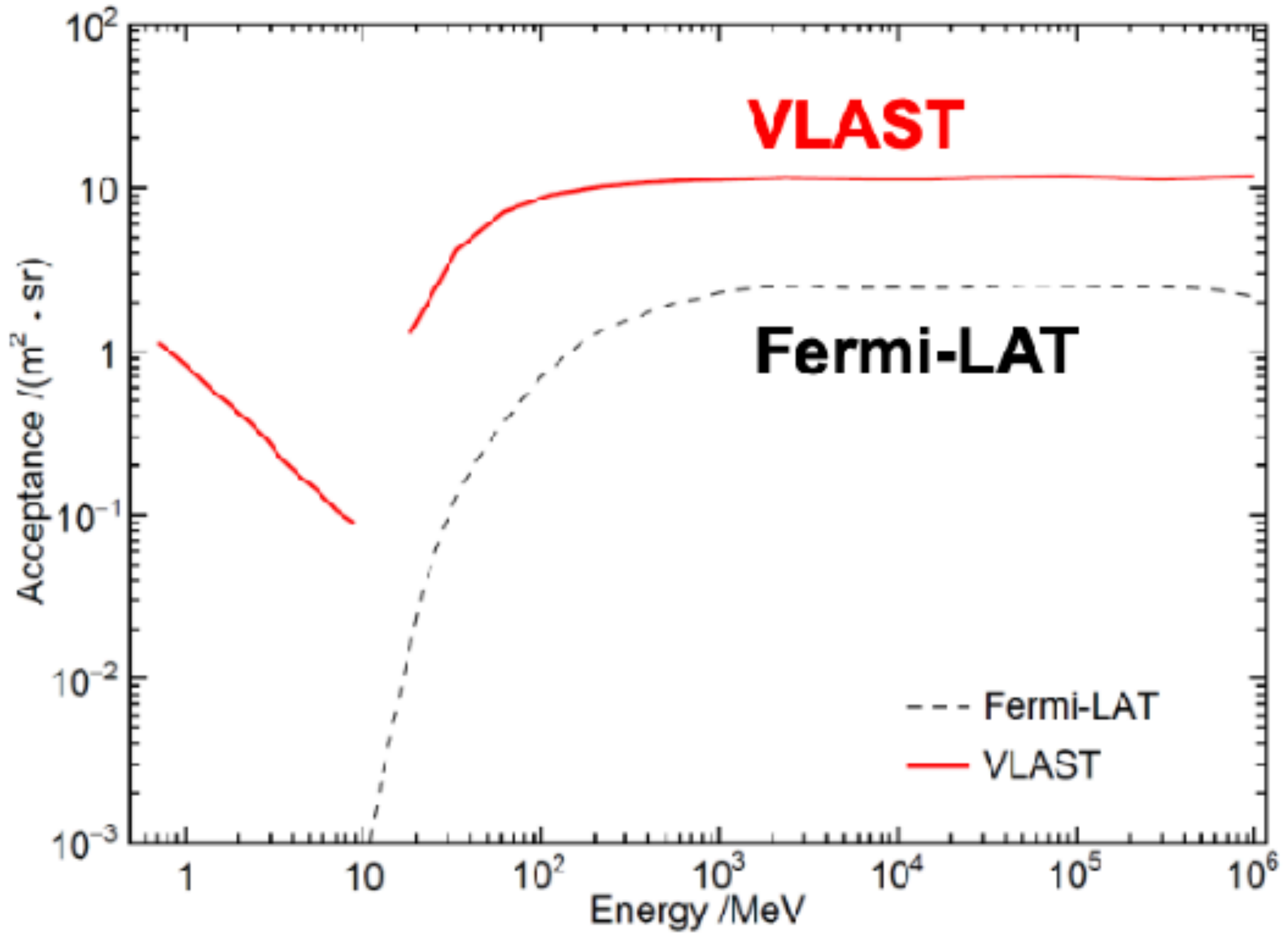

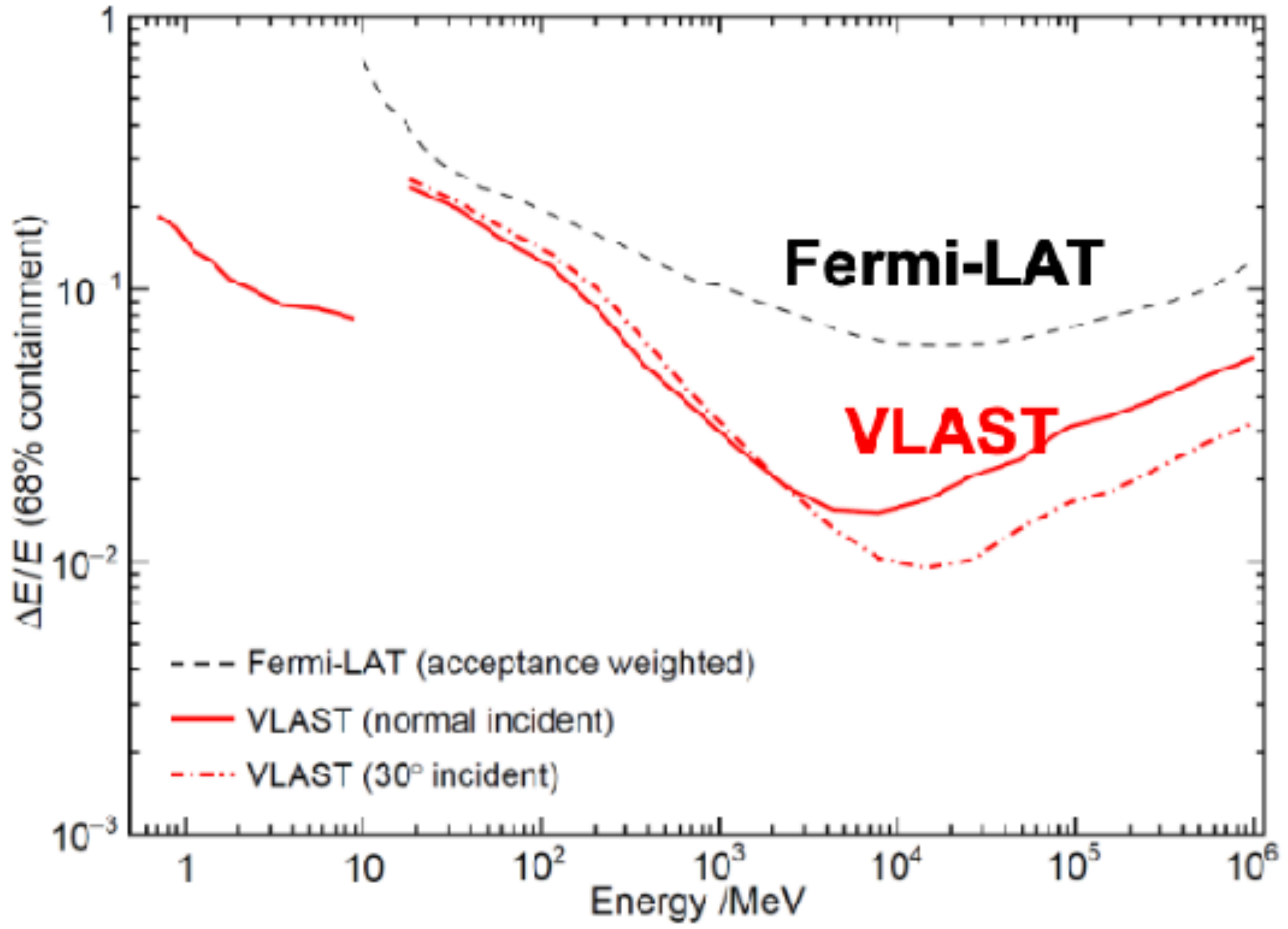

国内外正在运行或提议的一些相关空间探测项目

探测设施	主要探测对象	峰值接受度 (m² sr)	目前阶段	备注
Fermi-LAT	伽马射线	~ 2	在轨	量能器
悟空号	宇宙线、伽马	~ 0.3	在轨	
AMS-100	宇宙线、伽马	~100	初步概念	磁谱仪
先进粒子天文望远镜APT	伽马射线、宇宙线	~20	关键技术攻关	量能器
HERD	宇宙线	~4	关键技术攻关	
VLAST	伽马射线	~10	关键技术攻关	

新年快乐！ 谢谢大家！